Pacific Journal of Mathematics

NEW CONSTRUCTION OF FUNDAMENTAL DOMAINS FOR CERTAIN MOSTOW GROUPS

TIEHONG ZHAO

Volume 259 No. 1 September 2012

PACIFIC JOURNAL OF MATHEMATICS
Vol. 259, No. 1, 2012
dx.doi.org/10.2140/pjm.2012.259.209

NEW CONSTRUCTION OF FUNDAMENTAL DOMAINS FOR CERTAIN MOSTOW GROUPS

TIEHONG ZHAO

In this article, we give a new construction of fundamental polyhedra for certain Mostow groups in complex hyperbolic space. The shape of fundamental polyhedra is a natural generalization of the fundamental polyhedron for the sister of Eisenstein–Picard lattice.

1. Introduction

Mostow [1980] used the construction of fundamental domains to show that certain subgroups of PU(2, 1) are lattices. More recently, there has been a renewed interest in the construction of fundamental domains [Deraux et al. 2005; Falbel and Parker 2006; Falbel et al. 2011; Parker 2006; Zhao 2011]. In particular, Deraux, Falbel and Paupert gave a new construction of fundamental domains for some of the groups considered in [Mostow 1980]. In this paper we give another construction for the same groups. Our construction generalizes the fundamental domain we gave for the sister of the Eisenstein–Picard modular group. This generalization is in the same spirit as the construction of fundamental domains for Livné's groups given in [Parker 2006], which generalizes the construction of the domain for the Eisenstein–Picard modular group given in [Falbel and Parker 2006].

Mostow groups are generated by three complex reflections R_1, R_2, R_3, each of order $p = 3, 4, 5$. The complex lines fixed by three reflections are permuted by a map J of order 3, equivalently, $JR_iJ^{-1} = R_{i+1}$ (indices taken cyclically). So $\langle R_1, R_2, R_3\rangle$ is a normal subgroup of $\langle R_1, J\rangle$ with index at most 3. Moreover, the complex reflection R_i satisfies the braid relation $R_iR_jR_i = R_jR_iR_j$. Such groups are determined up to conjugation by a real parameter, which Mostow [1980] calls a phase shift, and denotes by φ. These groups have the property that $A_i = (JR_i^{-1}J)^2$ is also a complex reflection and there is a one to one correspondence between the phase shift parameter φ and the angle of this reflection A_i. In order for $\langle R_1, J\rangle$ to be discrete, the complex reflection A_i should have finite order and we take this order to be k. Following [Parker 2009], we use p and k rather than φ to specify the group $\langle R_1, J\rangle$.

MSC2010: primary 32Q45; secondary 51M10.
Keywords: Mostow groups, Poincaré polyhedron theorem, fundamental domains.

Most of the paper concerns the case $p = 3$ and for other values of p we will only make some remarks about how the construction needs to be modified; see Section 5. When $p = 3$ the values of k that lead to a lattice are exactly those for which there is an integer l so that $1/k + 1/l = \frac{1}{6}$ (see also the table in [Parker 2009, page 27]). In [Zhao 2011] we constructed a fundamental domain for the case $k = 6$. In this paper, we consider the case $k \geq 7$ and construct a fundamental domain whose shape is based on that of the domain for $k = 6$. The main difference is that the vertex at ∞ is replaced with a triangle in a complex line and we need to be careful when constructing geodesic cones to point this triangle. Our construction is inspired by the construction of Parker [2006], in the case $p \geq 7$ and $k = 2$, which are generalizations of the construction for $p = 6$ and $k = 2$ given in [Falbel and Parker 2006]. Again the main difference is that the vertex of ∞ is replaced with a triangle in a complex line.

Our fundamental polyhedron is a 4-dimensional domain, which is well defined by its boundary (the union of 3-cells is homeomorphic to S^3). Analogously to [Parker 2006], the basic construction is to take a complex line L_0 instead of ∞ fixed by $\Gamma_0 \subset \Gamma$ (where Γ is the group we consider) and the intersection of a fundamental domain for Γ_0 and a Dirichlet type domain under $\Gamma\backslash\Gamma_0$. Specifically, the Dirichlet type domain $D_{\Gamma\backslash\Gamma_0}(L_0)$ based at L_0 is the set of points in $\boldsymbol{H}^2_{\mathbb{C}}$ that are closer to L_0 than to any other complex line in the $\Gamma\backslash\Gamma_0$-orbit of L_0. The faces of $D_{\Gamma\backslash\Gamma_0}(L_0)$ are contained in *bisectors*, that is, the locus of points equidistant from a pair of complex lines; see Section 3A. Throughout the paper, the 3-dimensional (2-, 1- and 0-dimensional) skeletons of a polyhedron are called the *sides* (*faces*, *edges* and *vertices*) of the polyhedron, respectively. The vertices of our polyhedron are intersections of two complex lines. Many, but not all, edges are geodesic arcs. Most of the sides are contained in bisectors. Only two sides that are not contained in bisectors will be constructed; they are foliated by 2-dimensional geodesic cones. Each of the faces is contained either in totally geodesic submanifolds or in a *Giraud disk* or in a foliation by geodesics. Consider the group generated by the side-pairing maps of our polyhedron; we use an appropriate version of the Poincaré polyhedron theorem to show that our polyhedron is a fundamental domain and give a presentation for this group.

2. Describing the group

For background on complex hyperbolic geometry, we refer the reader to [Goldman 1999] as a general reference. We consider the complex hyperbolic triangle group generated by three complex reflections R_1, R_2, R_3 of order p with the property that there is an element J of order 3 so that

$$J^3 = I, \quad R_2 = JR_1J^{-1}, \quad R_3 = JR_2J^{-1} = J^{-1}R_1J. \tag{2-1}$$

We call $\langle R_1, R_2, R_3\rangle$ an *equilateral triangle group* if condition (2-1) is satisfied.

2A. ***The group*** Γ_k**.** Consider an equilateral complex hyperbolic triangle group defined as above. Up to conjugation, it may be parametrized by $\tau = \mathrm{tr}(R_1 J)$. For the sake of simplicity, we set $u = e^{2i\pi/3p}$. Using a suitable normalization, we may take the Hermitian form H to be

$$H = \begin{bmatrix} 2-u^3-\overline{u}^3 & (\overline{u}^2-u)\tau & (u^2-\overline{u})\overline{\tau} \\ (u^2-\overline{u})\overline{\tau} & 2-u^3-\overline{u}^3 & (\overline{u}^2-u)\tau \\ (\overline{u}^2-u)\tau & (u^2-\overline{u})\overline{\tau} & 2-u^3-\overline{u}^3 \end{bmatrix}; \tag{2-2}$$

see [Parker and Paupert 2009].

The elements R_1, R_2, R_3 and J then take the form

$$R_1 = \begin{bmatrix} u^2 & \tau & -u\overline{\tau} \\ 0 & \overline{u} & 0 \\ 0 & 0 & \overline{u} \end{bmatrix}, \qquad R_2 = \begin{bmatrix} \overline{u} & 0 & 0 \\ -u\overline{\tau} & u^2 & \tau \\ 0 & 0 & \overline{u} \end{bmatrix},$$

$$R_3 = \begin{bmatrix} \overline{u} & 0 & 0 \\ 0 & \overline{u} & 0 \\ \tau & -u\overline{\tau} & u^2 \end{bmatrix}, \qquad J = \begin{bmatrix} 0 & 0 & 1 \\ 1 & 0 & 0 \\ 0 & 1 & 0 \end{bmatrix},$$

as matrices in $\mathrm{SU}(H)$. As shown in [Parker 2009], having $|\tau| = 1$ is equivalent to Mostow's condition that the generators R_j and R_k satisfy the braid relation $R_j R_k R_j = R_k R_j R_k$ for $j \neq k$. Furthermore, following [Sauter 1990] we define $A_j = (JR_j^{-1}J)^2$ for $j = 1, 2, 3$, then A_j is a complex reflection or is conjugate to a vertical Heisenberg translation (see Proposition 4.1 of [Parker 2009]). In particular, if A_j is conjugate to a vertical Heisenberg translation then $\tau = -1$.

We focus our attention on considering the groups generated by three complex reflections of order 3 and so $u^3 = e^{2i\pi/3}$ is a cube root of unity. We follow the notation used in [Parker and Paupert 2009] and write $\tau = -e^{-2i\pi/3k}$ where k is an integer (and set $\tau = -1$ when $k = \infty$), and denote the corresponding group by Γ_k. We now give the generators as $R = (JR_1^{-1}J)^2$, $S = JR_1^{-1}$, $T = (JR_1^{-1})^2$ and $I_1 = JR_1^{-1}J$. Recall that the generators R, S, T, I_1 arise from the side-pairing maps of a fundamental domain constructed in [Zhao 2011], we call them *geometrical generators*. So the group Γ_k may be rewritten as $\langle R, S, T, I_1\rangle$. Our main result is the construction of a fundamental domain for Γ_k acting on complex hyperbolic space and a presentation of the group Γ_k.

2B. ***The stabilizer.*** In this section we will investigate the stabilizer subgroup of Γ_k preserving a complex line, which enables us to obtain the values of k as required.

In the case $k = 6$ [Zhao 2011], $\langle R, S, T\rangle$ is an isotropy group fixing a boundary point, so it is a cusp group. It is natural to ask what happens to the group

$\langle R, S, T\rangle \subset \Gamma_k$ for other values of k? To answer this we need to consider the location of the common eigenvector of R, S and T in $\mathbb{C}_H^{2,1}$ where $\mathbb{C}_H^{2,1}$ is the Hermitian symmetric complex vector space corresponding to the Hermitian matrix H.

From the above settings of generators, we see easily that $T = S^2$, which can simplify the group $\langle R, S, T\rangle$ to $\langle R, S\rangle = \langle R^{-1}S, S\rangle = \langle R_3, JR_1^{-1}\rangle$. It suffices to find a common eigenvector of R_3 and JR_1^{-1}. As matrices of $\mathrm{SU}(H)$,

$$R_3 = \begin{bmatrix} \overline{u} & 0 & 0 \\ 0 & \overline{u} & 0 \\ \tau & -u\overline{\tau} & u^2 \end{bmatrix} \quad \text{and} \quad JR_1^{-1} = \begin{bmatrix} 0 & 0 & u \\ \overline{u}^2 & -\overline{u}\tau & \overline{\tau} \\ 0 & u & 0 \end{bmatrix}.$$

By simple calculations, the common eigenvector of R_3 and JR_1^{-1} in $\mathbb{C}_H^{2,1}$ is

$$\boldsymbol{n} = \begin{bmatrix} u^2\overline{\tau} \\ \overline{u}^2\tau \\ -1 \end{bmatrix}.$$

In particular, $\boldsymbol{n}$ is the eigenvector of T that corresponds to its nonrepeated eigenvalue. More specifically, we say T is a complex reflection in the complex line with the polar vector $\boldsymbol{n}$. A *polar vector* to the complex line L is a vector $\boldsymbol{v}$ in $\mathbb{C}_H^{2,1}$ satisfying $\langle \boldsymbol{v}, z\rangle_H = 0$ for $z \in L$.

Using the Hermitian form (2-2), the following calculations enable us to know whether the eigenvector $\boldsymbol{n}$ is a negative, null or positive vector in $\mathbb{C}_H^{2,1}$. We have

$$\begin{aligned} \langle \boldsymbol{n}, \boldsymbol{n}\rangle &= \begin{bmatrix} \overline{u}^2\tau & u^2\overline{\tau} & -1 \end{bmatrix} H \begin{bmatrix} u^2\overline{\tau} \\ \overline{u}^2\tau \\ -1 \end{bmatrix} \\ &= 1 - u^3 + \overline{u}^6\tau^3 - \overline{u}^3\tau^3 + u^6\overline{\tau}^3 - u^3\overline{\tau}^3 + 1 - \overline{u}^3 \\ &= 2 - u^3 - \overline{u}^3 + (u^3 - \overline{u}^3)\tau^3 + (\overline{\tau}^3 - u^3)\overline{\tau}^3 \\ &= 3 + 2i\sin(2\pi/3)(\tau^3 - \overline{\tau}^3) \\ &= 3 - 2\sqrt{3}\sin(2\pi/k). \end{aligned}$$

From this, we get

$$\begin{aligned} \langle \boldsymbol{n}, \boldsymbol{n}\rangle > 0 &\Longleftrightarrow k > 6, \\ \langle \boldsymbol{n}, \boldsymbol{n}\rangle = 0 &\Longleftrightarrow k = 6, \\ \langle \boldsymbol{n}, \boldsymbol{n}\rangle < 0 &\Longleftrightarrow k < 6. \end{aligned}$$

For $k > 6$, $\boldsymbol{n}$ is a positive vector in $\mathbb{C}_H^{2,1}$, which turns out to be a polar vector to a complex line as required. Furthermore, the eigenvector $\boldsymbol{n}$ is a null vector when $k = 6$. As $\langle \boldsymbol{n}, \boldsymbol{n}\rangle$ tends to 0, the polar vector $\boldsymbol{n}$ degenerates to a point on the boundary of complex hyperbolic space as well. This limiting configuration

corresponds to a cusp of the corresponding lattice, which is conjugate to the sister of Eisenstein–Picard modular group [Zhao 2011].

2C. ***New normalization of*** $\boldsymbol{\Gamma_k}$**.** Calculations in complex hyperbolic space, in terms of the Hermitian form (2-2), have a tendency to become extremely complicated, which means that explicit constructions are rather difficult to obtain. We have to make a good choice of coordinates in order to give simple and explicit geometrical arguments on Γ_k. In what follows we choose the Hermitian matrix

$$H_0 = \begin{bmatrix} 1 & 0 & 0 \\ 0 & 1 & 0 \\ 0 & 0 & -1 \end{bmatrix}.$$

The corresponding Hermitian form in complex vector space $\mathbb{C}^{2,1}$ is defined by

$$\langle z, w\rangle = z_1\overline{w}_1 + z_2\overline{w}_2 - z_3\overline{w}_3,$$

where z and w are the column vectors $[z_1, z_2, z_3]^t$ and $[w_1, w_2, w_3]^t$ respectively. Thus we obtain, in nonhomogeneous coordinates, the complex ball

$$\boldsymbol{H}^2_{\mathbb{C}} = \{(z_1, z_2) \in \mathbb{C}^2 : |z_1|^2 + |z_2|^2 < 1\}.$$

The key point of our normalization is based on a geometric observation of the complex lines fixed by T and R respectively. In fact, it follows from the braid relation $R_1R_3R_1 = R_3R_1R_3$ that R commutes with T. Thus the complex lines fixed by T and R (denoted by $\mathscr{C}_1$ and $\mathscr{C}_2$ respectively) are orthogonal. We choose a new coordinate system of the complex ball, which makes $\mathscr{C}_1$ and $\mathscr{C}_2$ be on the z_1- and z_2-axis, specifically

$$\mathscr{C}_1 = \{(z_1, 0) \in \mathbb{C}^2 : |z_1| < 1\}, \tag{2-3}$$

$$\mathscr{C}_2 = \{(0, z_2) \in \mathbb{C}^2 : |z_2| < 1\}. \tag{2-4}$$

We now start to normalize the generators of Γ_k in the new system of coordinates. Before normalizing, we need to introduce two angle parameters,

$$\phi_1 = \pi/k, \tag{2-5}$$

$$\phi_2 = \pi/6 - \pi/k, \tag{2-6}$$

that play an important role in the normalization of the group Γ_k. Also, we shall give several numbers related to ϕ_1 and ϕ_2 in order to simplify expressions. We

remind the readers to keep these numbers in mind for convenience:

$$x_1 = \sqrt{\frac{\sin(\pi/6-\phi_1)}{\sin(\pi/6+\phi_1)}}, \tag{2-7}$$

$$x_2 = \sqrt{\frac{\sin(\pi/6-\phi_2)}{\sin(\pi/6+\phi_2)}}, \tag{2-8}$$

$$\rho = \sqrt{\frac{\sin(\pi/6-\phi_1/2)}{\cos(\phi_1/2)\sin(\pi/6+\phi_1)}}, \tag{2-9}$$

$$\lambda = \sqrt{\tan(\phi_1/2)\tan(\pi/6-\phi_1/2)}, \tag{2-10}$$

$$\mu = \sqrt{\frac{\tan(\phi_1/2)}{\tan(\pi/6-\phi_1/2)}}, \tag{2-11}$$

$$\delta = \sqrt{\frac{\tan(\phi_2/2)}{\tan(\pi/6-\phi_2/2)}}. \tag{2-12}$$

As matrices of SU(2, 1), the complex reflections R and T are given by

$$R = \begin{bmatrix} e^{4i\phi_1/3} & 0 & 0 \\ 0 & e^{-2i\phi_1/3} & 0 \\ 0 & 0 & e^{-2i\phi_1/3} \end{bmatrix},$$
$$T = \begin{bmatrix} e^{-2i\phi_2/3} & 0 & 0 \\ 0 & e^{4i\phi_2/3} & 0 \\ 0 & 0 & e^{-2i\phi_2/3} \end{bmatrix}. \tag{2-13}$$

We start by defining the vertices of our polyhedron to be the intersection of two complex lines. We consider two more complex lines, namely those fixed by R_1 and R_3, and denote them by $\mathscr{L}_1$ and $\mathscr{L}_3$ respectively.

(i) The vertices on $\mathscr{L}_1$ are

$$z_1 = \mathscr{L}_1 \cap \mathscr{C}_2, \quad z_2 = \mathscr{L}_1 \cap \mathscr{L}_3, \quad z_3 = \mathscr{L}_1 \cap R(\mathscr{L}_3).$$

(ii) The vertices on $T(\mathscr{L}_1)$ are

$$z_6 = T(\mathscr{L}_1) \cap \mathscr{C}_2, \quad z_4 = T(\mathscr{L}_1) \cap \mathscr{L}_3, \quad z_5 = T(\mathscr{L}_1) \cap R(\mathscr{L}_3).$$

(iii) The vertices on $\mathscr{C}_1$ are

$$z_7 = \mathscr{C}_1 \cap \mathscr{C}_2, \quad z_8 = \mathscr{C}_1 \cap \mathscr{L}_3, \quad z_9 = \mathscr{C}_1 \cap R(\mathscr{L}_3).$$

Proposition 2.1. *If z_j are defined by* (i), (ii) *and* (iii) *for $j = 1, 2, \ldots, 9$, then*

$$z_3 = R(z_2), \quad z_5 = R(z_4), \quad z_9 = R(z_8),$$
$$z_6 = T(z_1), \quad z_4 = T(z_2), \quad z_5 = T(z_3).$$

Proof. The braid relations $R_1R_2R_1 = R_2R_1R_2$ and $R_2R_3R_2 = R_3R_2R_3$ imply that R commutes with R_1 and that T commutes with R_3, respectively. As a consequence, we know that R commutes with TR_1T^{-1} and that T commutes with RR_3R^{-1}. It follows that $\mathscr{C}_1$ is orthogonal to $\mathscr{L}_3$ and $R(\mathscr{L}_3)$, and that $\mathscr{C}_2$ is orthogonal to $\mathscr{L}_1$ and $T(\mathscr{L}_1)$. Therefore, R preserves $\mathscr{C}_1$, $\mathscr{L}_1$ and $T(\mathscr{L}_1)$. Also, T preserves $\mathscr{C}_2$, $\mathscr{L}_3$ and $R(\mathscr{L}_3)$. The result now follows easily from definitions. □

We now start by investigating the coordinates of the complex lines $\mathscr{L}_1$ and $\mathscr{L}_3$ under the symmetry map J. Consider the triangle with the vertices z_2, z_3, z_4. First observe that J acts on the vertices with the property that $J(z_j) = z_{j+1}$ (with indices taken cyclically). To see this, note that it follows from $R_1(z_2) = R_3(z_2) = z_2$ and $J^3 = 1$ that

$$\begin{aligned} J(z_2) &= RR_3R_1(z_2) = R(z_2) = z_3, \\ J(z_4) &= JT(z_2) = J^{-1}R_1^{-1}J(z_2) = R_3^{-1}(z_2) = z_2, \\ J(z_3) &= JR(z_2) = J^{-1}R_1^{-1}R_3^{-1}(z_2) = J^{-1}(z_2) = z_4. \end{aligned}$$

Thus (z_2, z_3, z_4) is an equilateral triangle whose vertices, as vectors of $\mathbb{C}^{2,1}$, satisfy

$$\begin{aligned} \langle z_1, z_1\rangle = \langle z_2, z_2\rangle = \langle z_3, z_3\rangle, \\ |\langle z_1, z_2\rangle| = |\langle z_2, z_3\rangle| = |\langle z_3, z_1\rangle|. \end{aligned} \tag{2-14}$$

The condition (2-14) gives rise to parametrizations of complex lines $\mathscr{L}_1$ and $\mathscr{L}_3$, that are given, in terms of nonhomogeneous coordinates, by

$$\mathscr{L}_1 = \left\{\left(z_1, x_2e^{-i\phi_2}\right) \in \mathbb{C}^2 : |z_1| < \sqrt{1-x_2^2}\right\}, \tag{2-15}$$

$$\mathscr{L}_3 = \left\{\left(x_1e^{-i\phi_1}, z_2\right) \in \mathbb{C}^2 : |z_2| < \sqrt{1-x_1^2}\right\}. \tag{2-16}$$

As vectors of $\mathbb{C}^{2,1}$, these vertices are given by

$$\begin{aligned} z_1 &= \begin{bmatrix} 0 \\ x_2e^{-i\phi_2} \\ 1 \end{bmatrix}, \quad z_2 = \begin{bmatrix} x_1e^{-i\phi_1} \\ x_2e^{-i\phi_2} \\ 1 \end{bmatrix}, \quad z_3 = \begin{bmatrix} x_1e^{i\phi_1} \\ x_2e^{-i\phi_2} \\ 1 \end{bmatrix}, \\ z_4 &= \begin{bmatrix} x_1e^{-i\phi_1} \\ x_2e^{i\phi_2} \\ 1 \end{bmatrix}, \quad z_5 = \begin{bmatrix} x_1e^{i\phi_1} \\ x_2e^{i\phi_2} \\ 1 \end{bmatrix}, \quad z_6 = \begin{bmatrix} 0 \\ x_2e^{i\phi_2} \\ 1 \end{bmatrix}, \\ z_7 &= \begin{bmatrix} 0 \\ 0 \\ 1 \end{bmatrix}, \quad z_8 = \begin{bmatrix} x_1e^{-i\phi_1} \\ 0 \\ 1 \end{bmatrix}, \quad z_9 = \begin{bmatrix} x_1e^{i\phi_1} \\ 0 \\ 1 \end{bmatrix}. \end{aligned} \tag{2-17}$$

Recall that given a vector $\boldsymbol{v}$ with $\langle \boldsymbol{v}, \boldsymbol{v}\rangle > 0$, the complex reflection in the complex line with the polar vector $\boldsymbol{v}$ is given by

$$R_{v,\zeta}(z) = z + (\zeta - 1)\frac{\langle z, \boldsymbol{v}\rangle}{\langle \boldsymbol{v}, \boldsymbol{v}\rangle}\boldsymbol{v}, \tag{2-18}$$

where ζ is a complex number of absolute value one.

Observe that the polar vectors to the complex lines $\mathscr{L}_1$ and $\mathscr{L}_3$, denoted by $\boldsymbol{n}_1$ and $\boldsymbol{n}_3$ respectively, are given by

$$\boldsymbol{n}_1 = \begin{bmatrix} 0 \\ 1 \\ x_2 e^{i\phi_2} \end{bmatrix} \quad \text{and} \quad \boldsymbol{n}_3 = \begin{bmatrix} 1 \\ 0 \\ x_2 e^{i\phi_1} \end{bmatrix}.$$

Since R_1 and R_3 are complex reflections with order 3, we set $\zeta = u^3 = e^{2i\pi/3}$ and then have $\zeta - 1 = i\sqrt{3}e^{i\pi/3}$. Using the formula (2-18) together with the facts that $\langle \boldsymbol{n}_1, \boldsymbol{n}_1\rangle = 1 - x_2^2$ and $\langle \boldsymbol{n}_3, \boldsymbol{n}_3\rangle = 1 - x_1^2$, the complex reflections R_1 and R_3 are given explicitly as matrices of SU(2, 1) by

$$R_1 = \begin{bmatrix} \overline{u} & 0 & 0 \\ 0 & \dfrac{i(u^2+\overline{u})e^{-i\phi_2}}{2\sin\phi_2} & -\dfrac{i(u^2+\overline{u})\sqrt{1-4\sin^2\phi_2}\,e^{-i\phi_2}}{2\sin\phi_2} \\ 0 & \dfrac{i(u^2+\overline{u})\sqrt{1-4\sin^2\phi_2}\,e^{i\phi_2}}{2\sin\phi_2} & -\dfrac{i(u^2+\overline{u})e^{i\phi_2}}{2\sin\phi_2} \end{bmatrix},$$

$$R_3 = \begin{bmatrix} \dfrac{i(u^2+\overline{u})e^{-i\phi_1}}{2\sin\phi_1} & 0 & -\dfrac{i(u^2+\overline{u})\sqrt{1-4\sin^2\phi_1}\,e^{-i\phi_1}}{2\sin\phi_1} \\ 0 & \overline{u} & 0 \\ \dfrac{i(u^2+\overline{u})\sqrt{1-4\sin^2\phi_1}\,e^{i\phi_1}}{2\sin\phi_1} & 0 & -\dfrac{i(u^2+\overline{u})e^{i\phi_1}}{2\sin\phi_1} \end{bmatrix}.$$

The symmetry map J plays an important role in the construction. From the equality $J = RR_3R_1$ we obtain

$$J = e^{i(\phi_2-\phi_1+\pi)/3} \begin{bmatrix} \dfrac{e^{i\phi_1}}{2\sin\phi_1} & \dfrac{\sqrt{(1-4\sin^2\phi_1)(1-4\sin^2\phi_2)}}{4\sin\phi_1\sin\phi_2} & -\dfrac{\sqrt{1-4\sin^2\phi_1}}{4\sin\phi_1\sin\phi_2} \\ 0 & \dfrac{e^{-i\phi_2}}{2\sin\phi_2} & -\dfrac{\sqrt{1-4\sin^2\phi_2}\,e^{-i\phi_2}}{2\sin\phi_2} \\ \dfrac{\sqrt{1-4\sin^2\phi_1}\,e^{i\phi_1}}{2\sin\phi_1} & \dfrac{\sqrt{1-4\sin^2\phi_2}}{4\sin\phi_1\sin\phi_2} & -\dfrac{1}{4\sin\phi_1\sin\phi_2} \end{bmatrix}.$$

Now define, from the relations $S = JR_1^{-1}$, $I_1 = TR_1$, the remaining generators by

$$S = \frac{e^{-i\phi_2/3}}{2\sin\phi_1}\begin{bmatrix} 1 & 0 & -\sqrt{1-4\sin^2\phi_1} \\ 0 & -2\sin\phi_1 e^{i\phi_2} & 0 \\ \sqrt{1-4\sin^2\phi_1} & 0 & -1 \end{bmatrix}, \tag{2-19}$$

$$I_1 = \frac{e^{-i\phi_1/3}}{2\sin\phi_2}\begin{bmatrix} -2\sin\phi_2 e^{i\phi_1} & 0 & 0 \\ 0 & 1 & -\sqrt{1-4\sin^2\phi_2} \\ 0 & \sqrt{1-4\sin^2\phi_2} & -1 \end{bmatrix}. \tag{2-20}$$

3. A combinatorial polyhedron

In this section we construct a polyhedron D which we will prove later to be a fundamental domain for Γ_k in complex hyperbolic space. The polyhedron D is defined to be a 4-dimensional domain bounded by the sides we construct in Sections 3C–3E. Many (but not all) sides of D are contained in bisectors and the vertices are the same as defined in the previous section. The main difficulty of the construction occurs when dealing with the two sides that are not contained in bisectors, each of which is foliated by 2-dimensional cones. In order to have a global view of the polyhedron, we refer to Figures 9 and 10.

3A. ***Bisectors.*** Recall that a bisector is the locus of points in complex hyperbolic space that are equidistant from a given pair of points p and q in complex hyperbolic space and we denote it by $\mathcal{B}_{p,q}$. Using a normalization of p and q such that $\langle \boldsymbol{p}, \boldsymbol{p}\rangle = \langle \boldsymbol{q}, \boldsymbol{q}\rangle$, the bisector $\mathcal{B}_{p,q}$ (see Section 3.3 of [Parker 2006]) is defined as

$$\mathcal{B}_{p,q} = \{z \in \boldsymbol{H}^2_{\mathbb{C}} : |\langle z, \boldsymbol{p}\rangle| = |\langle z, \boldsymbol{q}\rangle|\}. \tag{3-1}$$

In fact, this definition of a bisector only depends on $\langle \boldsymbol{p}, \boldsymbol{p}\rangle = \langle \boldsymbol{q}, \boldsymbol{q}\rangle$ and not on whether this quantity is positive, negative or zero.

(a) If $\langle \boldsymbol{p}, \boldsymbol{p}\rangle = \langle \boldsymbol{q}, \boldsymbol{q}\rangle = 0$, i.e., the points p and q are on the boundary of complex hyperbolic space, then we use the *Busemann functions* with respect to p and q (as defined in Section 4.1.2 of [Goldman 1999]) instead of the standard distance function.

(b) If $\langle \boldsymbol{p}, \boldsymbol{p}\rangle = \langle \boldsymbol{q}, \boldsymbol{q}\rangle > 0$, i.e., the points p and q are outside of complex hyperbolic space, then we say $\mathcal{B}_{p,q}$ is equidistant from the complex lines $\mathcal{C}_p$ and $\mathcal{C}_q$ with polar vectors p and q respectively. In other words, for each $z \in \mathcal{B}_{p,q}$ the distance from z to the closest point of $\mathcal{C}_p$ is the same as the distance from z to the closest point of $\mathcal{C}_q$. In Section 3C we will use this characterization of bisectors.

The points p and q lie on a unique complex line Σ, called the *complex spine* of the bisector $\mathcal{B}_{p,q}$. There is a geodesic σ in Σ that is equidistant from our pair of points with respect to the natural Poincaré metric on Σ. This geodesic

is called the *spine*. This still makes sense when p and q lie on the boundary of $\boldsymbol{H}^2_{\mathbb{C}}$ or lie outside it: we may define the spine as the locus of points in Σ fixed by an involution interchanging p and q. In particular, the (complex) spine may be outside of complex hyperbolic space. Bisectors are not totally geodesic (there are no totally geodesic real hypersurfaces in complex hyperbolic space), but can be described in terms of a foliation by totally geodesic subspaces in two different ways. First there is the slice decomposition; see [Mostow 1980]. Let Π_Σ denote the orthogonal projection onto Σ, then the bisector is the preimage of σ under Π_Σ. Each fiber of this map, i.e., each complex line that is the preimage of a point of σ, is a *slice* of our bisector. Bisectors enjoy another decomposition into totally real, totally geodesic submanifolds, which we call the *meridians*; see [Goldman 1999]. Each meridian is a Lagrangian plane that contains the spine σ, the bisector is the union of all its meridians.

An example in the ball model is the *standard* bisector

$$\mathcal{B}_0 = \{(z_1, z_2) \in \boldsymbol{H}^2_{\mathbb{C}} : z_1 \in \mathbb{C}, \operatorname{Im} z_2 = 0\}$$

in nonhomogeneous coordinates, which is equidistant from the points $p = (0, i/2)$ and $q = (0, -i/2)$, for instance.

Together the slices and meridians give *geographical coordinates* on the bisector. In the unit ball model (compare [Falbel and Parker 2006]), in geographical coordinates, the standard bisector $\mathcal{B}_0$ is parametrized by

$$\left\{ \begin{bmatrix} re^{i\alpha} \\ s \\ 1 \end{bmatrix} : \alpha \in [-\pi/2, \pi/2),\, s \in [-1, 1],\, r \in \left[-\sqrt{1-s^2}, \sqrt{1-s^2}\right] \right\}. \tag{3-2}$$

The spine, slices and meridians of $\mathcal{B}_0$ are given in the next proposition in terms of geographical coordinates.

Proposition 3.1. *The standard bisector with coordinates* (r, s, α) *is given by* (3-2). *Furthermore*,

(i) *the spine of* $\mathcal{B}_0$ *is given by* $r = 0$;

(ii) *the slices of* $\mathcal{B}_0$ *are given by* $s = s_0$ *for fixed* $s_0 \in [-1, 1]$;

(iii) *the meridians of* $\mathcal{B}_0$ *are given by* $\alpha = \alpha_0$ *for fixed* $\alpha_0 \in [-\pi/2, \pi/2)$.

The intersection of two or more bisectors can be very complicated, in general it is not necessarily connected or contained in a totally geodesic subspace. We adopt the following notation and recall several results that allow us to understand the intersection of bisectors.

Definition 3.2. Let $\mathcal{B}_1$ and $\mathcal{B}_2$ denote bisectors with complex spines Σ_1 and Σ_2 respectively.

(i) We call $\mathcal{B}_1$ and $\mathcal{B}_2$ *cospinal* if $\Sigma_1 = \Sigma_2$.

(ii) We call $\mathcal{B}_1$ and $\mathcal{B}_2$ *coequidistant* if $\Sigma_1 \cap \Sigma_2$ does not lie in their real spines.

(iii) We call $\mathcal{B}_1$ and $\mathcal{B}_2$ *cotranchal* if they share a common slice.

(iv) We call $\mathcal{B}_1$ and $\mathcal{B}_2$ *comeridional* if they share a common meridian.

The following result allows us to understand bisector intersections in terms of their slice decompositions.

Proposition 3.3 [Mostow 1980]. *Let $\mathcal{B}$ be a bisector and $\mathcal{C}$ be a complex line such that $\mathcal{B} \cap \mathcal{C} \neq \varnothing$, then $\mathcal{C} \subset \mathcal{B}$ (in which case $\mathcal{C}$ is a slice of $\mathcal{B}$) or $\mathcal{C} \cap \mathcal{B}$ is a hypercycle in $\mathcal{C}$. In the ball model a hypercycle is an arc of a Euclidean circle intersecting the boundary.*

We remark that a hypercycle in $\mathcal{C}$ is a curve with a constant geodesic curvature (i.e., the magnitude of the mean curvature is constant). In particular, unless the two bisectors share a common slice, Proposition 3.3 implies that each connected component of the intersection $\mathcal{B}_1 \cap \mathcal{B}_2$ is a disk that is foliated by arcs of circles. It can be proven that the intersection has at most two connected components. If the bisectors are coequidistant, there is a remarkable result due to Giraud.

Proposition 3.4 [Giraud 1921; Goldman 1999]. *Let $\mathcal{B}_1$ and $\mathcal{B}_2$ be two coequidistant bisectors with complex spines Σ_1 and Σ_2 respectively, then their intersection is a smooth disk, moreover there exists one (and no more) bisector containing $\mathcal{B}_1 \cap \mathcal{B}_2$ other than $\mathcal{B}_1$ and $\mathcal{B}_2$.*

This intersection is not totally geodesic. We call it a *Giraud disk*. We can find the third bisector passing through a Giraud disk by the following procedure. Suppose that $\mathcal{B}_1$ and $\mathcal{B}_2$ is a pair of coequidistant bisectors with respective complex (real respectively) spines Σ_1 and Σ_2 (σ_1 and σ_2 respectively), then we denote $\Sigma_1 \cap \Sigma_2$ by p_0 and the images of p_0 under the reflections in σ_1 and σ_2 by p_2 and p_1. Then the third bisector equidistant from p_1 and p_2 passes through the intersection $\mathcal{B}_1 \cap \mathcal{B}_2$.

Four of the bisectors we use to construct the polyhedron D have a very simple descriptions. These four bisectors come in two cospinal pairs, the complex spines being the coordinate axes. We write down these bisectors and some of the points for (2-17) that are contained in the corresponding bisector:

Bisector	Definition	Vertices on spine	Other vertices
$\mathcal{B}_{78}$	$\arg(z_1) = -\phi_1$	z_7, z_8	z_1, z_2, z_4, z_6
$\mathcal{B}_{79}$	$\arg(z_1) = \phi_1$	z_7, z_9	z_1, z_3, z_5, z_6
$\mathcal{B}_{17}$	$\arg(z_2) = -\phi_2$	z_1, z_7	z_2, z_3, z_8, z_9
$\mathcal{B}_{67}$	$\arg(z_2) = \phi_2$	z_6, z_7	z_4, z_5, z_8, z_9

3B. ***Orthogonal projection onto*** $\mathbb{C}$***-lines.*** We need a few technical lemmas about the orthogonal projection onto a $\mathbb{C}$-line that we shall use in what follows. The sketch of the proof follows from geometric facts.

Lemma 3.5 [Thompson 2010, Lemma 1.2.17]. *Let* $\Pi_{\mathscr{C}}$ *be the orthogonal projection of complex hyperbolic space onto a* $\mathbb{C}$*-line* $\mathscr{C}$ *and* γ *be a geodesic. Then the image* $\Pi_{\mathscr{C}}(\gamma)$ *is either*

- *a single point, or*
- *an arc of a geometric circle in* $\mathscr{C}$*.*

In particular, if $\gamma \cap \mathscr{C} \neq \varnothing$*, then* $\Pi_{\mathscr{C}}(\gamma)$ *is the geodesic segment between the projection of the endpoints of* γ *at infinity.*

Proof. Using the ball model of $\boldsymbol{H}^2_{\mathbb{C}}$, we may assume that $\mathscr{C} = \{(z_1, 0) |\ z_1 \in \mathbb{C}\}$. This makes the orthogonal projection linear, that is $\Pi_{\mathscr{C}}(z_1, z_2) = z_1$. We also assume that γ is not contained in any complex line $z_1 =$ constant, otherwise γ can be projected to a single point as required.

Recall that a $\mathbb{C}$-line is the nonempty intersection of a complex projective line with $\boldsymbol{H}^2_{\mathbb{C}}$ and a geodesic is the locus of a quadratic equation with respect to the real and imaginary parts of coordinates in a $\mathbb{C}$-line. From this, we see that $\Pi_{\mathscr{C}}(\gamma)$ is the locus of a quadratic equation with respect to $\operatorname{Re} z_1$ and $\operatorname{Im} z_1$, which is a geometric circle in $\mathscr{C}$.

To see this is true for a general $\mathbb{C}$-line, recall that a $\mathbb{C}$-line is an embedded copy of $\boldsymbol{H}^1_{\mathbb{C}}$ and that an element of $\mathrm{PU}(2, 1)$ sending a $\mathbb{C}$-line to another is an isometry of $\boldsymbol{H}^1_{\mathbb{C}}$. Holomorphic isometries of $\boldsymbol{H}^1_{\mathbb{C}}$ are Möbius transformations, which send circles to circles. For the particular case of $\gamma \cap \mathscr{C} \neq \varnothing$, the result follows from the fact that a linear projection sends any straight line to another one. □

Lemma 3.6 [Thompson 2010, Lemma 1.2.19]. *Let* γ *be a geodesic and* p, q *be two points on* γ*. Then the geodesic segment* $[p, q]$ *projects to a shorter arc of a geometric circle on a coordinate axis.*

Proof. Let $\mathscr{C}_0$ be a complex line containing the geodesic γ. Using the ball model of $\boldsymbol{H}^2_{\mathbb{C}}$, we know that $\mathscr{C}_0$ is an embedded copy of Poincaré disk in $\boldsymbol{H}^2_{\mathbb{C}}$. We consider the extensions $\overline{\gamma}$ and $\overline{\mathscr{C}_0}$ of γ and $\mathscr{C}_0$ to projective space. There is an involution fixing S^3 (the boundary of $\partial \boldsymbol{H}^2_{\mathbb{C}}$) in $\mathbb{C}^2$,

$$(z_1, z_2) \to \left(\frac{z_1}{|z_1|^2 + |z_2|^2}, \frac{z_2}{|z_1|^2 + |z_2|^2} \right),$$

which preserves the extension $\overline{\gamma}$ and swaps the two parts $\overline{\gamma} \backslash \gamma$ and γ. It follows (like in Poincaré disk) that γ is shorter than $\overline{\gamma} \backslash \gamma$ with respect to the Euclidean metric. By Lemma 3.5, the projection of γ is a geometrical circle in a $\mathbb{C}$-line. Furthermore, the orthogonal projection on a coordinate axis is linear, which implies

that it preservers angles. As a consequence, the projection sends the geodesic γ to a shorter arc of a geometric circle. So does each geodesic segment $[p, q]$. □

3C. ***The core sides.*** In this section we define two core sides $\mathcal{S}_c$ and $\mathcal{S}'_c$ of the polyhedron D contained in a bisector $\mathcal{B}_c$, called the *core bisector*, which is equidistant from two complex lines $\mathcal{C}_1$ and $I_1^{-1}(\mathcal{C}_1)$ as explained in Section 3A (compare [Zhao 2011]). We call the union of two sides $\mathcal{S}_c$ and $\mathcal{S}'_c$ the *core prism*, and denote it by $\mathcal{P}_c$ (see Figure 4 for a schematic view). The other sides of D are foliated by 2-dimensional cones. Four of these sides are contained in the bisectors given in the previous section. Analogously to the sister of the Eisenstein–Picard lattice (the case $k = 6$), the noncompact sides of the fundamental polyhedron arise from the limiting configuration resulting from the top triangle converging to an ideal vertex. In other words, the polyhedron is the geodesic cone over the faces of the core prism to the ideal point which is a cusp of lattice; see [Zhao 2011].

The core bisector and its neighbors. Let $\boldsymbol{n}_0$ denote the polar vector to the complex line $\mathcal{C}_1$ and denote by $I_1^{-1}(\boldsymbol{n}_0)$ its image under by I_1^{-1}, these are

$$\boldsymbol{n}_0 = \begin{bmatrix} 0 \\ 1 \\ 0 \end{bmatrix} \quad \text{and} \quad I_1^{-1}(\boldsymbol{n}_0) = \frac{e^{i\phi_1/3}}{2\sin\phi_2} \begin{bmatrix} 0 \\ 1 \\ \sqrt{1-4\sin^2\phi_2} \end{bmatrix}.$$

We denote by $\mathcal{B}_c$ the bisector equidistant from $\boldsymbol{n}_0$ and $I_1^{-1}(\boldsymbol{n}_0)$. The condition that $\langle \boldsymbol{n}_0, \boldsymbol{n}_0 \rangle = \langle I_1^{-1}(\boldsymbol{n}_0), I_1^{-1}(\boldsymbol{n}_0) \rangle = 1$ enables us to give the definition of $\mathcal{B}_c$ as characterized in (3-1).

Definition 3.7. The bisector $\mathcal{B}_c$ is defined in nonhomogeneous coordinates by

$$\mathcal{B}_c = \left\{ (z_1, z_2) \in \boldsymbol{H}^2_{\mathbb{C}} : 2\sin\phi_2 |z_2| = \left| z_2 - \sqrt{1-4\sin^2\phi_2} \right| \right\}. \tag{3-3}$$

Observe that $\mathcal{C}_2$ is the complex spine of $\mathcal{B}_c$ spanned by $\boldsymbol{n}_0$ and $I_1^{-1}(\boldsymbol{n}_0)$. Since the complex lines $\mathcal{L}_1$ and $T(\mathcal{L}_1)$ are both orthogonal to the complex line $\mathcal{C}_2$, it follows that the spine of $\mathcal{B}_c$ passes through a pair of vertices z_1 and z_6 by the slice decomposition for bisectors; see Figure 1.

We shall explore the spine of $\mathcal{B}_c$ in order to give the parametrization in terms of geographical coordinates (r, s, α). In the coordinate system $(x, y) = (\operatorname{Re} z, \operatorname{Im} z)$ in $\mathbb{C}$, the Poincaré disk is $\{(x, y) |\, x^2 + y^2 < 1\}$ and the spine σ_0 turns out to be

$$\left(x - 1/\sqrt{1-4\sin^2\phi_2}\right)^2 + y^2 = \frac{4\sin^2\phi_2}{1-4\sin^2\phi_2}. \tag{3-4}$$

This is a circle centered at

$$\left(\frac{1}{\sqrt{1-4\sin^2\phi_2}}, 0 \right) \text{ with radius } \frac{2\sin\phi_2}{\sqrt{1-4\sin^2\phi_2}}.$$

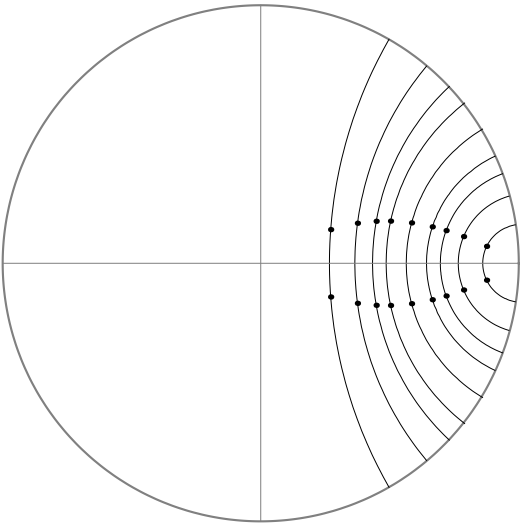

Figure 1. Configuration of the spines of the bisector $\mathcal{B}_c$ and z_1, z_6 on the complex spine $\mathcal{C}_2$ for $k = 7, 8, 9, 10, 12, 15, 18, 24, 42$. Here the spines get closer to the origin as k gets larger.

The spine σ_0 intersects the x-axis at the point $(\mu, 0)$. Then we apply a Möbius transformation ψ mapping $(\mu, 0)$ to the origin in the Poincaré disk, for example

$$\psi(z) = \frac{z-\mu}{1-\mu z}.$$

Equation (3-4) becomes $|z+\mu| = |z-\mu|$ under the map ψ, so it describes the y-axis. Defining a map C in SU(2, 1) by

$$C = \begin{bmatrix} e^{-i\pi/6} & 0 & 0 \\ 0 & e^{i\pi/3}/(1-\mu^2) & e^{-i\pi/6}\mu/(1-\mu^2) \\ 0 & e^{i\pi/3}\mu/(1-\mu^2) & e^{-i\pi/6}/(1-\mu^2) \end{bmatrix},$$

we see that C maps the spine of standard bisector $\mathcal{B}_0$ to the spine of $\mathcal{B}_c$ and furthermore the geographical coordinates on $\mathcal{B}_c$ turn out to be obtained from $\mathcal{B}_0$.

Definition 3.8. The bisector $\mathcal{B}_c$ is given in terms of geographical coordinates (r, s, α) by

$$\left\{ \begin{bmatrix} \sqrt{1-\mu^2}\, r e^{i\alpha} \\ \mu + is \\ 1 + i\mu s \end{bmatrix} : \begin{array}{l} \alpha \in [-\pi/2, \pi/2), \quad s \in [-1, 1], \\ r \in \left[-\sqrt{1-s^2}, \sqrt{1-s^2}\right] \end{array} \right\}. \tag{3-5}$$

We start to define the sides $\mathcal{S}_c$ and $\mathcal{S}'_c$ in geographical coordinates. As described in [Falbel et al. 2011], we will discuss the triangular face with the vertices z_2, z_3, z_4

on the intersection $\mathcal{B}_c \cap S^{-1}(\mathcal{B}_c)$ in terms of two slice s-parameters. We give the details for this face on $\mathcal{B}_c \cap S^{-1}(\mathcal{B}_c)$ and the others follow similarly.

Proposition 3.9. *The part of $\mathcal{B}_c \cap S^{-1}(\mathcal{B}_c)$ outside $T^{-1}(\mathcal{B}_c)$, $R^{-1}S(\mathcal{B}_c)$, $S(\mathcal{B}_c)$ forms a triangular face of the core prism, see Figure 2. In terms of geographical coordinates (r_0, s_0, α_0) on $\mathcal{B}_c$ and (r_1, s_1, α_1) on $S^{-1}(\mathcal{B}_c)$ this face is given by*

$$-\lambda \le s_0 \le \lambda, \quad -\lambda \le s_1 \le \lambda, \quad -2\lambda \le s_0 - s_1 \le 0. \tag{3-6}$$

Moreover, the boundary of this triangle admits the following description in geographical coordinates.

(i) *Points of $\mathcal{B}_c \cap S^{-1}(\mathcal{B}_c) \cap T^{-1}(\mathcal{B}_c)$ are given by $s_0 = -\lambda$.*

(ii) *Points of $\mathcal{B}_c \cap S^{-1}(\mathcal{B}_c) \cap S(\mathcal{B}_c)$ are given by $s_1 = \lambda$.*

(iii) *Points of $\mathcal{B}_c \cap S^{-1}(\mathcal{B}_c) \cap R^{-1}S(\mathcal{B}_c)$ are given by $s_0 - s_1 = 0$.*

We remark that none of the triple intersections (i)–(iii) in Proposition 3.9 are contained in a geodesic; refer to Lemma 3.18. Before we prove Proposition 3.9, we need to explore the intersection $\mathcal{B}_c \cap S^{-1}(\mathcal{B}_c)$ in terms of two slices parameters s_0, s_1 and see how it intersects the neighboring bisectors $T^{-1}(\mathcal{B}_c)$, $R^{-1}S(\mathcal{B}_c)$ and $S(\mathcal{B}_c)$.

Proposition 3.10. *Consider the geographical coordinates (r_0, s_0, α_0) on $\mathcal{B}_c$ and (r_1, s_1, α_1) on $S^{-1}(\mathcal{B}_c)$. Points on $\mathcal{B}_c \cap S^{-1}(\mathcal{B}_c)$ may be uniquely expressed in terms of s_0 and s_1; see Figure 2. The range of these parameters is determined by the inequality*

$$\left| \frac{(1 + i\mu s_0)(\mu + i s_1) - 2\sin\phi_1 e^{i\phi_2}(1 + i\mu s_1)(\mu + i s_0)}{\sqrt{(1-\mu^2)(1 - 4\sin^2\phi_1)}(\mu + i s_1)} \right| < \sqrt{1 - s_0^2}.$$

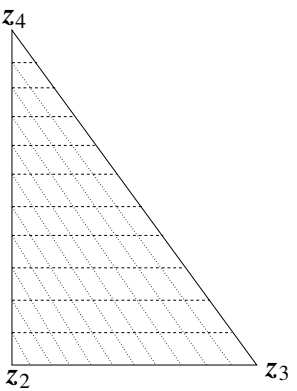

Figure 2. Schematic picture of the triangular face $\mathcal{F}_{234}$. The level sets of s_0 are dashed lines and the level sets of s_1 are dotted lines.

The other coordinates are given by

$$r_0 e^{i\alpha_0} = \frac{(1+i\mu s_0)(\mu+is_1) - 2\sin\phi_1 e^{i\phi_2}(1+i\mu s_1)(\mu+is_0)}{\sqrt{(1-\mu^2)(1-4\sin^2\phi_1)}(\mu+is_1)}, \tag{3-7}$$

$$r_1 e^{i\alpha_1} = \frac{(1+i\mu s_1)(\mu+is_0) - 2\sin\phi_1 e^{-i\phi_2}(1+i\mu s_0)(\mu+is_1)}{\sqrt{(1-\mu^2)(1-4\sin^2\phi_1)}(\mu+is_0)}. \tag{3-8}$$

Proof. In geographical coordinates, points of $\mathcal{B}_c \cap S^{-1}(\mathcal{B}_c)$ are given by

$$\begin{bmatrix} 1 & 0 & -\sqrt{1-4\sin^2\phi_1} \\ 0 & -2\sin\phi_1 e^{-i\phi_2} & 0 \\ \sqrt{1-4\sin^2\phi_1} & 0 & -1 \end{bmatrix} \begin{bmatrix} \sqrt{1-\mu^2} r_1 e^{i\alpha_1} \\ \mu+is_1 \\ 1+i\mu s_1 \end{bmatrix}$$

$$= \begin{bmatrix} \sqrt{1-\mu^2} r_1 e^{i\alpha_1} - \sqrt{1-4\sin^2\phi_1}(1+i\mu s_1) \\ -2\sin\phi_1 e^{-i\phi_2}(\mu+is_1) \\ \sqrt{1-4\sin^2\phi_1}\sqrt{1-\mu^2} r_1 e^{i\alpha_1} - (1+i\mu s_1) \end{bmatrix}.$$

Since this must equal

$$\begin{bmatrix} \sqrt{1-\mu^2} r_0 e^{i\alpha_0} \\ \mu+is_0 \\ 1+i\mu s_0 \end{bmatrix}$$

as homogeneous coordinates, we get the equalities

$$\frac{-2\sin\phi_1 e^{-i\phi_2}(\mu+is_1)}{\sqrt{1-4\sin^2\phi_1}\sqrt{1-\mu^2} r_1 e^{i\alpha_1} - (1+i\mu s_1)} = \frac{\mu+is_0}{1+i\mu s_0}, \tag{3-9}$$

$$\frac{\sqrt{1-\mu^2} r_1 e^{i\alpha_1} - \sqrt{1-4\sin^2\phi_1}(1+i\mu s_1)}{-2\sin\phi_1 e^{-i\phi_2}(\mu+is_1)} = \frac{\sqrt{1-\mu^2} r_0 e^{i\alpha_0}}{\mu+is_0}. \tag{3-10}$$

Rearranging (3-9) gives

$$r_1 e^{i\alpha_1} = \frac{(1+i\mu s_1)(\mu+is_0) - 2\sin\phi_1 e^{-i\phi_2}(1+i\mu s_0)(\mu+is_1)}{\sqrt{(1-\mu^2)(1-4\sin^2\phi_1)}(\mu+is_0)}.$$

To find $r_0 e^{i\alpha_0}$ we just use this formula to substitute for $r_1 e^{i\alpha_1}$ in (3-10).

In order to be in $\mathcal{B}_c$ we must have $r_0^2 < 1 - s_0^2$. Using (3-7) we can obtain the range of s_0, s_1 as required. □

Analogously, we describe $\mathcal{B}_c \cap S(\mathcal{B}_c)$ and $\mathcal{B}_c \cap R^{-1}S(\mathcal{B}_c)$.

Proposition 3.11. *Consider the geographical coordinates (r_0, s_0, α_0) on $\mathcal{B}_c$ and (r_2, s_2, α_2) on $S(\mathcal{B}_c)$. Points on $\mathcal{B}_c \cap S(\mathcal{B}_c)$ may be uniquely expressed in terms of s_0 and s_2. The range of these parameters is determined by the inequality*

$$\left| \frac{(1+i\mu s_0)(\mu+is_2) - 2\sin\phi_1 e^{-i\phi_2}(1+i\mu s_2)(\mu+is_0)}{\sqrt{(1-\mu^2)(1-4\sin^2\phi_1)}(\mu+is_2)} \right| < \sqrt{1-s_0^2}.$$

The other coordinates are given by

$$r_0 e^{i\alpha_0} = \frac{(1+i\mu s_0)(\mu+is_2) - 2\sin\phi_1 e^{-i\phi_2}(1+i\mu s_2)(\mu+is_0)}{\sqrt{(1-\mu^2)(1-4\sin^2\phi_1)}(\mu+is_2)}, \tag{3-11}$$

$$r_2 e^{i\alpha_2} = \frac{(1+i\mu s_2)(\mu+is_0) - 2\sin\phi_1 e^{i\phi_2}(1+i\mu s_0)(\mu+is_2)}{\sqrt{(1-\mu^2)(1-4\sin^2\phi_1)}(\mu+is_0)}. \tag{3-12}$$

Proposition 3.12. *Consider the geographical coordinates* (r_0, s_0, α_0) *on* $\mathcal{B}_c$ *and* (r_3, s_3, α_3) *on* $R^{-1}S(\mathcal{B}_c)$. *Points on* $\mathcal{B}_c \cap R^{-1}S(\mathcal{B}_c)$ *may be uniquely expressed in terms of* s_0 *and* s_3; *see Figure 3. The range of these parameters is determined by the inequality*

$$\left| \frac{(1+i\mu s_0)(\mu+is_3) - 2\sin\phi_1 e^{-i\phi_2}(1+i\mu s_3)(\mu+is_0)}{\sqrt{(1-\mu^2)(1-4\sin^2\phi_1)}(\mu+is_3)} \right| < \sqrt{1-s_0^2}.$$

The other coordinates are given by

$$r_0 e^{i\alpha_0} = \frac{e^{-2i\phi_1}[(1+i\mu s_0)(\mu+is_3) - 2\sin\phi_1 e^{-i\phi_2}(1+i\mu s_3)(\mu+is_0)]}{\sqrt{(1-\mu^2)(1-4\sin^2\phi_1)}(\mu+is_3)}, \tag{3-13}$$

$$r_3 e^{i\alpha_3} = \frac{(1+i\mu s_3)(\mu+is_0) - 2\sin\phi_1 e^{i\phi_2}(1+i\mu s_0)(\mu+is_3)}{\sqrt{(1-\mu^2)(1-4\sin^2\phi_1)}(\mu+is_0)}. \tag{3-14}$$

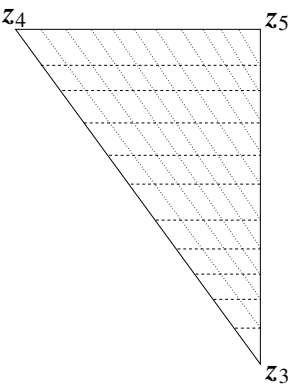

Figure 3. Schematic picture of the triangular face $\mathcal{F}_{345}$. The level sets of s_0 are dashed lines and the level sets of s_2 are dotted lines.

Proof. In geographical coordinates, points of $\mathcal{B}_c \cap R^{-1}S(\mathcal{B}_c)$ are given by

$$\begin{bmatrix} u^2 e^{i\phi_2} & 0 & -u^2\sqrt{1-4\sin^2\phi_1}e^{i\phi_2} \\ 0 & 2\overline{u}\sin\phi_1 & 0 \\ -\overline{u}\sqrt{1-4\sin^2\phi_1}e^{-i\phi_2} & 0 & \overline{u}e^{-i\phi_2} \end{bmatrix} \begin{bmatrix} \sqrt{1-\mu^2}r_3 e^{i\alpha_3} \\ \mu + is_3 \\ 1+i\mu s_3 \end{bmatrix}$$
$$= \begin{bmatrix} e^{-2i\phi_1}[\sqrt{1-\mu^2}r_3 e^{i\alpha_3} - \sqrt{1-4\sin^2\phi_1}(1+i\mu s_3)] \\ -2\sin\phi_1 e^{i\phi_2}(\mu+is_3) \\ \sqrt{1-4\sin^2\phi_1}\sqrt{1-\mu^2}r_3 e^{i\alpha_3} - (1+i\mu s_1) \end{bmatrix} = \begin{bmatrix} \sqrt{1-\mu^2}r_0 e^{i\alpha_0} \\ \mu+is_0 \\ 1+i\mu s_0 \end{bmatrix}.$$

The result follows as before. □

Corollary 3.13. *In terms of geographical coordinates* (r_1, s_1, α_1) *on* $S^{-1}(\mathcal{B}_c)$ *and* (r_2, s_2, α_2) *on* $S(\mathcal{B}_c)$, *points of* $\mathcal{B}_c \cap S^{-1}(\mathcal{B}_c) \cap S(\mathcal{B}_c)$ *are given by* $s_1 = \lambda$ *or* $s_2 = -\lambda$.

Proof. Points of $\mathcal{B}_c \cap S^{-1}(\mathcal{B}_c) \cap S(\mathcal{B}_c)$ are given by

$$r_0 e^{i\alpha_0} = \frac{(1+i\mu s_0)(\mu+is_1) - 2\sin\phi_1 e^{i\phi_2}(1+i\mu s_1)(\mu+is_0)}{\sqrt{(1-\mu^2)(1-4\sin^2\phi_1)}(\mu+is_1)}$$
$$= \frac{(1+i\mu s_0)(\mu+is_2) - 2\sin\phi_1 e^{-i\phi_2}(1+i\mu s_2)(\mu+is_0)}{\sqrt{(1-\mu^2)(1-4\sin^2\phi_1)}(\mu+is_2)}.$$

From this we find

$$e^{i\phi_2}[\mu(1-s_1s_2) + i(s_2+\mu s_1)] = e^{-i\phi_2}[\mu(1-s_1s_2) + i(s_1+\mu s_2)].$$

Hence $s_1 + s_2 = 0$ and $s_1 = \lambda$. □

Corollary 3.14. *In geographical coordinates* (r_0, s_0, α_0) *on* $\mathcal{B}_c$, (r_1, s_1, α_1) *on* $S^{-1}(\mathcal{B}_c)$ *and* (r_3, s_3, α_3) *on* $R^{-1}S(\mathcal{B}_c)$, *points of* $\mathcal{B}_c \cap S^{-1}(\mathcal{B}_c) \cap R^{-1}S(\mathcal{B}_c)$ *are given by* $s_0 - s_1 = 0$ *and* $s_0 - s_3 = 0$.

Proof. Points of $\mathcal{B}_c \cap S^{-1}(\mathcal{B}_c) \cap R^{-1}S(\mathcal{B}_c)$ are given by

$$r_0 e^{i\alpha_0} = \frac{(1+i\mu s_0)(\mu+is_1) - 2\sin\phi_1 e^{i\phi_2}(1+i\mu s_1)(\mu+is_0)}{\sqrt{(1-\mu^2)(1-4\sin^2\phi_1)}(\mu+is_1)}$$
$$= \frac{e^{-2i\phi_1}[(1+i\mu s_0)(\mu+is_3) - 2\sin\phi_1 e^{-i\phi_2}(1+i\mu s_3)(\mu+is_0)]}{\sqrt{(1-\mu^2)(1-4\sin^2\phi_1)}(\mu+is_3)}.$$

From this we find

$$\frac{e^{i\pi/6}(1+i\mu s_1)}{\mu+is_1} - \frac{e^{-i\pi/6}(1+i\mu s_3)}{\mu+is_3} = \frac{i(1+i\mu s_0)}{\mu+is_0}.$$

Comparing the real and imaginary parts yields

$$\sqrt{3}\mu(s_1 - s_3) + 2s_1s_3 = s_0(s_1 + s_3),$$
$$\sqrt{3}s_0(s_1 - s_3) + 2\mu s_0 = \mu(s_1 + s_3).$$

Eliminating s_3 from the above equations, we obtain a quadratic equation with respect to s_1,

$$(\sqrt{3}s_0 - \mu)s_1^2 + (2\mu s_0 + \sqrt{3}\mu^2 - \sqrt{3}s_0^2)s_1 - \mu s_0(\sqrt{3}\mu + s_0) = 0.$$

It follows immediately that two solutions are

$$s_1 = s_0 \quad \text{and} \quad s_1 = \frac{\mu(\sqrt{3}\mu + s_0)}{\mu - \sqrt{3}s_0}.$$

The latter is impossible since $s_1 > \lambda$. Thus $s_0 = s_1 = s_3$. □

Similarly, we state the result on the intersection of $\mathcal{B}_c \cap S(\mathcal{B}_c)$.

Proposition 3.15. *The part of $\mathcal{B}_c \cap S(\mathcal{B}_c)$ outside $T(\mathcal{B}_c)$, $RS^{-1}(\mathcal{B}_c)$, $S^{-1}(\mathcal{B}_c)$ forms a triangular face of the core prism, see Figure 3. In terms of geographical coordinates (r_0, s_0, α_0) on $\mathcal{B}_c$ and (r_2, s_2, α_2) on $S(\mathcal{B}_c)$ this face is given by*

$$-\lambda \le s_0 \le \lambda, \quad -\lambda \le s_2 \le \lambda, \quad 0 \le s_0 - s_2 \le 2\lambda. \tag{3-15}$$

The boundary of this triangle admits the following description in geographical coordinates:

(i) *Points of $\mathcal{B}_c \cap S(\mathcal{B}_c) \cap T(\mathcal{B}_c)$ are given by $s_0 = \lambda$.*

(ii) *Points of $\mathcal{B}_c \cap S(\mathcal{B}_c) \cap S^{-1}(\mathcal{B}_c)$ are given by $s_2 = -\lambda$.*

(iii) *Points of $\mathcal{B}_c \cap S(\mathcal{B}_c) \cap RS^{-1}(\mathcal{B}_c)$ are given by $s_0 - s_2 = 0$.*

Proof. The map S sends $(r_0, s_0, \alpha_0) \in \mathcal{B}_c$ to $(r_2, s_2, \alpha_2) \in S(\mathcal{B}_c)$. So S sends points on $\mathcal{B}_c \cap S^{-1}(\mathcal{B}_c) \cap T^{-1}(\mathcal{B}_c)$ given by $s_0 = -\lambda$ to points on $\mathcal{B}_c \cap S(\mathcal{B}_c) \cap S^{-1}(\mathcal{B}_c)$ given by $s_2 = -\lambda$. Analogously, the map R preserves the s_0-slices of $\mathcal{B}_c$ and sends $(r_3, s_3, \alpha_3) \in R^{-1}S(\mathcal{B}_c)$ to $(r_2, s_2, \alpha_2) \in S(\mathcal{B}_c)$. As in the proof of Corollary 3.14, points of $\mathcal{B}_c \cap S^{-1}(\mathcal{B}_c) \cap R^{-1}S(\mathcal{B}_c)$ are given by $s_0 - s_3 = 0$, which implies that points of $\mathcal{B}_c \cap S(\mathcal{B}_c) \cap RS^{-1}(\mathcal{B}_c)$ satisfy $s_0 - s_2 = 0$ as required. □

We now investigate the intersection of $\mathcal{B}_c$ with its images under T and T^{-1}.

Lemma 3.16. *The bisectors $\mathcal{B}_c$ and $T^{-1}(\mathcal{B}_c)$ have a common slice corresponding to $s_0 = -\lambda$ in terms of geographical coordinates (r_0, s_0, α_0) on $\mathcal{B}_c$.*

Likewise, $\mathcal{B}_c$ and $T(\mathcal{B}_c)$ have a common slice $s_0 = \lambda$ in geographical coordinates.

Proof. Points of $\mathcal{B}_c$ are given by $2\sin\phi_2|z_2| = |z_2 - \sqrt{1-4\sin^2\phi_2}|$ and points of $T^{-1}(\mathcal{B}_c)$ are given by $2\sin\phi_2|z_2| = |z_2 - \sqrt{1-4\sin^2\phi_2}e^{-2i\phi_2}|$. The common solution of these equations is $z_2 = x_2 e^{-i\phi_2}$. In geographical coordinates this is

$$\frac{\mu + is_0}{1 + i\mu s_0} = x_2 e^{-i\phi_2}$$

and since $s_0 \in [-1, 1]$, we obtain that $s_0 = -\lambda$. □

The vertices. We have already seen the vertices z_i $(i = 1, 2, \ldots, 6)$ of D lying on the slices $\mathcal{L}_1$ and $T(\mathcal{L}_1)$ of $\mathcal{B}_c$. We now list them again as the intersection of $\mathcal{B}_c$ with images of $\mathcal{B}_c$ under suitable elements in the stabilizer of $\mathcal{C}_1$ and discuss their nonhomogeneous coordinates and geographical coordinates.

(i) The vertices on the slice $\mathcal{L}_1 = \mathcal{B}_c \cap T^{-1}(\mathcal{B}_c)$ correspond to $s = -\lambda$. Let z_1 be the intersection of the spine of $\mathcal{B}_c$ with $\mathcal{L}_1$. The other vertices are given by

$$z_2 = \mathcal{B}_c \cap T^{-1}(\mathcal{B}_c) \cap S^{-1}(\mathcal{B}_c) \cap R^{-1}S(\mathcal{B}_c),$$
$$z_3 = \mathcal{B}_c \cap T^{-1}(\mathcal{B}_c) \cap S(\mathcal{B}_c) \cap RS^{-1}(\mathcal{B}_c).$$

(ii) The vertices on the slice $T(\mathcal{L}_1) = \mathcal{B}_c \cap T(\mathcal{B}_c)$ correspond to $s = \lambda$. Let z_6 be the intersection of the spine of $\mathcal{B}_c$ with $T(\mathcal{L}_1)$. The other vertices are given by

$$z_4 = \mathcal{B}_c \cap T(\mathcal{B}_c) \cap S^{-1}(\mathcal{B}_c) \cap R^{-1}S(\mathcal{B}_c),$$
$$z_5 = \mathcal{B}_c \cap T(\mathcal{B}_c) \cap S(\mathcal{B}_c) \cap RS^{-1}(\mathcal{B}_c).$$

In nonhomogeneous coordinates and geographical coordinates of the vertices z_i are given as follows, where the parameters $\phi_1, \phi_2, x_1, x_2, \rho, \lambda$ are defined in (2-5)–(2-10):

	z_1	z_2	r	s	α
z_1	0	$x_2e^{-i\phi_2}$	0	$-\lambda$	
z_2	$x_1e^{-i\phi_1}$	$x_2e^{-i\phi_2}$	ρ	$-\lambda$	$-3\phi_1/2$
z_3	$x_1e^{i\phi_1}$	$x_2e^{-i\phi_2}$	ρ	$-\lambda$	$\phi_1/2$
z_4	$x_1e^{-i\phi_1}$	$x_2e^{i\phi_2}$	ρ	λ	$-\phi_1/2$
z_5	$x_1e^{i\phi_1}$	$x_2e^{i\phi_2}$	ρ	λ	$3\phi_1/2$
z_6	0	$x_2e^{i\phi_2}$	0	λ	

The edges. We now characterize the edges of the core prism. Let $\gamma_{jk} = \gamma_{kj}$ denote the edge of D with the vertices z_j and z_k as endpoints. More specifically, we give them by the intersection of three bisectors:

$$\gamma_{12} = \mathcal{B}_c \cap T^{-1}(\mathcal{B}_c) \cap \mathcal{B}_{78}, \qquad \gamma_{24} = \mathcal{B}_c \cap S^{-1}(\mathcal{B}_c) \cap \mathcal{B}_{78},$$
$$\gamma_{13} = \mathcal{B}_c \cap T^{-1}(\mathcal{B}_c) \cap \mathcal{B}_{79}, \qquad \gamma_{35} = \mathcal{B}_c \cap S(\mathcal{B}_c) \cap \mathcal{B}_{79},$$
$$\gamma_{23} = \mathcal{B}_c \cap T^{-1}(\mathcal{B}_c) \cap S^{-1}(\mathcal{B}_c), \qquad \gamma_{34} = \mathcal{B}_c \cap S(\mathcal{B}_c) \cap S^{-1}(\mathcal{B}_c),$$

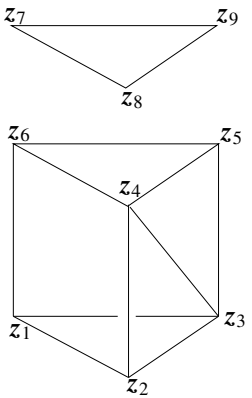

Figure 4. The core prism $\mathcal{P}_c$ contained in $\mathcal{B}_c$ and the geodesic triangle on the complex line $\mathcal{C}_1$.

$$\gamma_{46} = \mathcal{B}_c \cap T(\mathcal{B}_c) \cap \mathcal{B}_{78},$$
$$\gamma_{56} = \mathcal{B}_c \cap T(\mathcal{B}_c) \cap \mathcal{B}_{79},$$
$$\gamma_{45} = \mathcal{B}_c \cap T(\mathcal{B}_c) \cap S(\mathcal{B}_c).$$

In what follows, we give them in geographical coordinates. The geodesic edges are listed in Lemma 3.17 while the nongeodesic edges are given in Lemma 3.18. We recall the numbers ρ and λ defined in (2-9) and (2-10).

Lemma 3.17. (i) *The edge γ_{16} is contained in the spine of $\mathcal{B}_c$.*

(ii) *The edge γ_{12} is a geodesic arc, given in geographical coordinates by*

$$0 \le r_0 \le \rho, \quad s_0 = -\lambda, \quad \alpha_0 = -3\phi_1/2.$$

(iii) *The edge γ_{13} is a geodesic arc, given in geographical coordinates by*

$$0 \le r_0 \le \rho, \quad s_0 = -\lambda, \quad \alpha_0 = \phi_1/2.$$

(iv) *The edge γ_{46} is a geodesic arc, given in geographical coordinates by*

$$0 \le r_0 \le \rho, \quad s_0 = \lambda, \quad \alpha_0 = -\phi_1/2.$$

(v) *The edge γ_{56} is a geodesic arc, given in geographical coordinates by*

$$0 \le r_0 \le \rho, \quad s_0 = \lambda, \quad \alpha_0 = 3\phi_1/2.$$

Proof. Part (i) holds by construction. We now prove (ii) and the other parts follow similarly. The edge γ_{12} is defined to be the intersection of $\mathcal{B}_c \cap T^{-1}(\mathcal{B}_c) \cap \mathcal{B}_{78}$. It follows that the edge is contained in the slice of $\mathcal{B}_c$ with $s_0 = -\lambda$ by Lemma 3.16.

Following the definition of $\mathcal{B}_{78}$, we see that

$$\arg(z_1) = \arg\left(\frac{e^{i\alpha_0}}{1-i\tan(\phi_1/2)}\right) = -\phi_1,$$

which implies that $\alpha_0 = -3\phi_1/2$. Therefore this edge is a geodesic arc since it is contained in both a Lagrangian plane and a complex line. Moreover, we know that $r_0 = 0$ at z_1 and $r_0 = \rho$ at z_2. □

We describe the edges that are not contained in geodesics.

Lemma 3.18. (i) *The edge γ_{24} is given in the coordinates (r_0, s_0, α_0) of $\mathcal{B}_c$ by*

$$r_0 e^{i\alpha_0} = \frac{2\sin\phi_2 e^{-i\phi_1}(1+i\mu s_0)}{\sqrt{(1-\mu^2)(1-4\sin^2\phi_1)}},$$

where $s_0 \in [-\lambda, \lambda]$ and it is not contained in a geodesic.

(ii) *The edge γ_{34} is given in the coordinates (r_0, s_0, α_0) of $\mathcal{B}_c$ by*

$$r_0 e^{i\alpha_0} = \frac{2\sin\phi_2(1-i\mu s_0)}{\sqrt{(1-\mu^2)(1-4\sin^2\phi_1)}},$$

where $s_0 \in [-\lambda, \lambda]$ and it is not contained in a geodesic.

(iii) *The edge γ_{35} is given in the coordinates (r_0, s_0, α_0) of $\mathcal{B}_c$ by*

$$r_0 e^{i\alpha_0} = \frac{2\sin\phi_2 e^{i\phi_1}(1+i\mu s_0)}{\sqrt{(1-\mu^2)(1-4\sin^2\phi_1)}},$$

where $s_0 \in [-\lambda, \lambda]$ and it is not contained in a geodesic.

(iv) *The edge γ_{23} is given in the coordinates (r_0, s_0, α_0) of $\mathcal{B}_c$ by $s_0 = -\lambda$ and*

$$r_0 e^{i\alpha_0} = \frac{(1-i\mu\lambda)(\mu+is_1) - 2\sin\phi_1 e^{i\phi_2}(1+i\mu s_1)(\mu-i\lambda)}{\sqrt{(1-\mu^2)(1-4\sin^2\phi_1)}(\mu+is_1)},$$

where $s_1 \in [-\lambda, \lambda]$ and it is not contained in a geodesic.

(v) *The edge γ_{45} is given in the coordinates (r_0, s_0, α_0) of $\mathcal{B}_c$ by $s_0 = \lambda$ and*

$$r_0 e^{i\alpha_0} = \frac{(1+i\mu\lambda)(\mu+is_2) - 2\sin\phi_1 e^{-i\phi_2}(1+i\mu s_2)(\mu+i\lambda)}{\sqrt{(1-\mu^2)(1-4\sin^2\phi_1)}(\mu+is_2)},$$

where $s_2 \in [-\lambda, \lambda]$ and it is not contained in a geodesic.

Proof. We now prove (i) and the others follow similarly. Point (i) follows by substituting $s_1 = s_0$ in (3-7) and using the fact that z_2 and z_4 correspond to $s_0 = -\lambda$ and $s_0 = \lambda$ respectively. In particular, we see that neither s_0 nor α_0 is constant on this edge. This implies that this edge cannot be contained in a geodesic. □

The faces. In order to define the sides $\mathcal{S}_c$ and $\mathcal{S}'_c$ contained in $\mathcal{B}_c$, it suffices to describe their faces. We denote them by $\mathcal{F}_{ijk}$ or $\mathcal{F}_{ijkl}$, where i, j, k and l are the indices of the vertices of the face. We repeat the previous result and summarize them again.

(i) There are two $\mathbb{C}$-planar faces $\mathcal{F}_{123}$ and $\mathcal{F}_{456}$. The boundary of $\mathcal{F}_{123}$ is equal to $\gamma_{12} \cup \gamma_{13} \cup \gamma_{23}$ and the boundary of $\mathcal{F}_{456}$ is $\gamma_{46} \cup \gamma_{56} \cup \gamma_{45}$.

(ii) Two triangular faces $\mathcal{F}_{234}$ and $\mathcal{F}_{345}$ are contained in Giraud disks, namely the intersections $\mathcal{B}_c \cap S^{-1}(\mathcal{B}_c)$ and $\mathcal{B}_c \cap S(\mathcal{B}_c)$ respectively. The boundary of $\mathcal{F}_{234}$ is $\gamma_{23} \cup \gamma_{34} \cup \gamma_{24}$ and the boundary of $\mathcal{F}_{345}$ is $\gamma_{34} \cup \gamma_{45} \cup \gamma_{35}$.

(iii) Three quadrilateral faces $\mathcal{F}_{1246}$, $\mathcal{F}_{1346}$ and $\mathcal{F}_{1356}$ are foliated by geodesics. More precisely, given a fixed $s_0 \in [-\lambda, \lambda]$, the slice s_0 intersects the face $\mathcal{F}_{1246}$ (respectively $\mathcal{F}_{1346}$ and $\mathcal{F}_{1356}$) in a geodesic, one of whose endpoints is lying at γ_{16} and the other is lying at γ_{24} (respectively γ_{34} and γ_{35}). The boundary of $\mathcal{F}_{1246}$ is $\gamma_{12} \cup \gamma_{24} \cup \gamma_{46} \cap \gamma_{16}$, the boundary of $\mathcal{F}_{1346}$ is $\gamma_{13} \cup \gamma_{34} \cup \gamma_{46} \cap \gamma_{16}$ and the boundary of $\mathcal{F}_{1356}$ is $\gamma_{13} \cup \gamma_{35} \cup \gamma_{56} \cap \gamma_{16}$.

Remark. The face $\mathcal{F}_{1246}$ (or $\mathcal{F}_{1356}$), by construction, is exactly contained in the intersection of $\mathcal{B}_c$ with $\mathcal{B}_{78}$ (or $\mathcal{B}_{79}$). To prove this, it suffices to show that $z \in \mathcal{B}_c$ lies in a slice $s_0 \in [-\lambda, \lambda]$ if and only if $\arg(z_2) = \text{constant} \in [-\phi_2, \phi_2]$. That follows immediately from the equation

$$\arg(z_2) = \arg\Big(\frac{\mu + is}{1 + i\mu s}\Big).$$

To this end, we give the definitions of $\mathcal{S}_c$ and $\mathcal{S}'_c$. These follow from their boundaries, $\partial\mathcal{S}_c = \mathcal{F}_{1246} \cup \mathcal{F}_{1346} \cup \mathcal{F}_{123} \cup \mathcal{F}_{234}$ and $\partial\mathcal{S}'_c = \mathcal{F}_{1346} \cup \mathcal{F}_{1356} \cup \mathcal{F}_{456} \cup \mathcal{F}_{345}$.

Definition 3.19. The side $\mathcal{S}_c$ is made up of those points (r_0, s_0, α_0) of $\mathcal{B}_c$ with

(i) $-\lambda \le s_0 \le \lambda$,

(ii) $\arctan(\mu s_0) - \phi_1 \le \alpha_0 \le -\arctan(\mu s_0)$,

(iii) (r_0, s_0, α_0) outside of $S^{-1}(\mathcal{B}_c)$.

We have shown that a point (r_0, s_0, α_0) in the intersection $\mathcal{B}_c \cap S^{-1}(\mathcal{B}_c)$ needs to satisfy the formula (3-7). Comparing with two sides of equality in (3-7), it follows that the ratio between the imaginary part and real part of the right side of (3-7) is equal to $\tan\alpha_0$, which makes s_1 a function $f(s_0, \alpha_0)$ of s_0 and α_0. Thus the condition (iii) can be written in terms of geographical coordinates as

$$r_0 \le \left| \frac{(1 + i\mu s_0)(\mu + is_1) - 2\sin\phi_1 e^{i\phi_2}(1 + i\mu s_1)(\mu + is_0)}{\sqrt{(1-\mu^2)(1 - 4\sin^2\phi_1)}(\mu + is_1)} \right|$$

by replacing s_1 with $f(s_0, \alpha_0)$.

Definition 3.20. The side $\mathcal{S}'_c$ is made up of those points (r_0, s_0, α_0) of $\mathcal{B}_c$ with

(i) $-\lambda \le s_0 \le \lambda$,

(ii) $-\arctan(\mu s_0) \le \alpha_0 \le \arctan(\mu s_0) + \phi_1$,

(iii) (r_0, s_0, α_0) outside of $S(\mathcal{B}_c)$.

Condition (iii) follows from the same argument as (iii) of Definition 3.19.

3D. ***Sides of prism type.*** In this section we define four sides of the polyhedron D. These sides are contained in bisectors, denoted by $\mathcal{S}_{17}, \mathcal{S}_{67}, \mathcal{S}_{78}$ and $\mathcal{S}_{79}$, each of whose indices is the same as its corresponding bisector. A simple description of these sides is a triangular prism whose top and bottom faces are respectively contained in different slices of a bisector.

The sides $\mathcal{S}_{78}$ and $\mathcal{S}_{79}$. For these sides, we only need to describe the side $\mathcal{S}_{78}$ and the other follows similarly since $\mathcal{B}_{79} = R(\mathcal{B}_{78})$.

It suffices to define the boundary of $\mathcal{S}_{78}$ which is contained in the bisector $\mathcal{B}_{78}$.

• We define the edge γ_{78} to be the geodesic segment between z_7 and z_8 that is contained in the spine of $\mathcal{B}_{78}$.

• In terms of the slice decomposition, the faces $\mathcal{F}_{167}$ and $\mathcal{F}_{248}$ are respectively contained in two of the slices of $\mathcal{B}_{78}$.

• In terms of the meridian decomposition, the faces $\mathcal{F}_{1278}$ and $\mathcal{F}_{4678}$ are respectively contained in two of the meridians of $\mathcal{B}_{78}$. In order to see this, we verify that $\arg(z_1) = \arg(z_2) = -\phi_2$ and $\arg(z_4) = \arg(z_6) = \phi_2$ for the vertices defined in (2-17). In other words, the vertices z_1, z_2 lie on a meridian and the vertices z_4, z_6 lie on another meridian.

• The face $\mathcal{F}_{1246}$ is contained in the intersection of $\mathcal{B}_{78}$ and $\mathcal{B}_c$. A point (z_1, z_2) on the intersection of $\mathcal{B}_{78} \cap \mathcal{B}_c$ is given in nonhomogeneous coordinates by

$$\arg(z_1) = -\phi_1, \quad 2\sin\phi_2|z_2| = \left|z_2 - \sqrt{1 - 4\sin^2\phi_2}\right|.$$

Finally, a point $z = (z_1, z_2)$ of $\mathcal{B}_{78}$ lies outside of $\mathcal{B}_c$, (the point z is closer to $\mathcal{C}_1$ than to $I_1^{-1}(\mathcal{C}_1)$) if and only if

$$\arg(z_1) = -\phi_1, \quad 2\sin\phi_2|z_2| < \left|z_2 - \sqrt{1 - 4\sin^2\phi_2}\right|.$$

From the above we give the definitions of $\mathcal{S}_{78}$ and $\mathcal{S}_{79}$ in nonhomogeneous coordinates.

Definition 3.21. The side $\mathcal{S}_{78}$ is made up of those points (z_1, z_2) of $\mathcal{B}_{78}$ with

$$\arg(z_1) = -\phi_1, \quad |z_1| \le x_1, \quad -\phi_2 \le \arg(z_2) \le \phi_2,$$
$$2\sin\phi_2|z_2| \le \left|z_2 - \sqrt{1 - 4\sin^2\phi_2}\right|.$$

Definition 3.22. The side $\mathcal{S}_{79}$ is made up of those points (z_1, z_2) of $\mathcal{B}_{79}$ with

$$\arg(z_1) = \phi_1, \quad |z_1| \le x_1, \quad -\phi_2 \le \arg(z_2) \le \phi_2,$$
$$2\sin\phi_2 |z_2| \le \left|z_2 - \sqrt{1 - 4\sin^2\phi_2}\right|.$$

The sides $\mathcal{S}_{17}$ and $\mathcal{S}_{67}$. These two sides are respectively contained in two bisectors which are cospinal and cotranchal. They have a common slice $\mathcal{C}_1$ and a common complex spine $\mathcal{C}_2$.

We begin with defining the common face of $\mathcal{S}_{17}$ and $\mathcal{S}_{67}$, namely the face $\mathcal{F}_{789}$. We have known that the edges γ_{78} and γ_{79} are geodesic segments contained in the spines of $\mathcal{B}_{78}$ and $\mathcal{B}_{79}$ respectively. We also define the edge γ_{89} to be the geodesic segment between z_8 and z_9. In order to see this, we need to consider the action of S in the complex line $\mathcal{C}_1$. Observe that the map S preserves $\mathcal{C}_1$ and $S^2 = T$ acts on $\mathcal{C}_1$ as the identity. From this, we see that the map S restricted to $\mathcal{C}_1$ is order of 2 and is given explicitly by

$$S_{|\mathcal{C}_1} : z \longmapsto \frac{z - \sqrt{1-4\sin^2\phi_1}}{\sqrt{1-4\sin^2\phi_1}\, z - 1}.$$

By calculations, we see that S swaps z_8 and z_9 and fixes the point $(\delta, 0)$. It follows that S preserves the geodesic passing through z_8, z_9 and rotates about the point $(\delta, 0)$ with angle π. So we define the face $\mathcal{F}_{789}$ to be the geodesic triangle with the vertices z_7, z_8, z_9 in the complex line $\mathcal{C}_1$; see Figure 5.

In order to define $\mathcal{S}_{17}$ and $\mathcal{S}_{67}$, it remains to describe two faces $\mathcal{F}_{2389}$ and $\mathcal{F}_{4589}$.

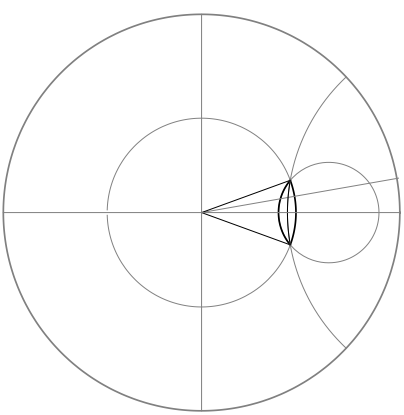

Figure 5. The face $\mathcal{F}_{789}$ is the geodesic triangle drawn by thin black lines. The orthogonal projection of γ_{23} (and γ_{45}) onto $\mathcal{C}_1$ is the bold arc contained in $\mathcal{F}_{789}$ while the projection of γ_{34} is the bold arc outside.

- We denote by $\alpha = \arg(z_1)$ and so the meridians of $\mathcal{B}_{17}$ and $\mathcal{B}_{67}$ correspond to α being constant.
- The projection of a meridian α onto $\mathcal{C}_1$ is a straight line passing through the origin with angle α.
- For each $\alpha \in [-\phi_1, \phi_1]$, we denote by $\boldsymbol{p}_0^\alpha$ the intersection of this straight line with the edge γ_{89}. Furthermore, we denote by $\boldsymbol{p}_1^\alpha$ and $\boldsymbol{p}_2^\alpha$ the intersection of the meridian α with the edges γ_{23} and γ_{45} respectively.

We denote by $[z, w]$ the geodesic segment between z and w in $\boldsymbol{H}^2_{\mathbb{C}}$ and define the faces $\mathcal{F}_{2389}$ and $\mathcal{F}_{4589}$ as

$$\mathcal{F}_{2389} = \bigcup_{\alpha\in[-\phi_1,\phi_1]} [\boldsymbol{p}_0^\alpha, \boldsymbol{p}_1^\alpha] \quad \text{and} \quad \mathcal{F}_{4589} = \bigcup_{\alpha\in[-\phi_1,\phi_1]} [\boldsymbol{p}_0^\alpha, \boldsymbol{p}_2^\alpha].$$

The following notation is used to simplify the expressions of $\mathcal{S}_{17}$ and $\mathcal{S}_{67}$. We call a *dihedral angle region* the domain enclosed by two different slices and meridians of a bisector. Two dihedral angle regions are defined by

$$\mathfrak{D}_{17} = \{(z_1, z_2) : -\phi_1 \le \arg(z_1) \le \phi_1, \arg(z_2) = -\phi_2, |z_2| \le x_2\},$$
$$\mathfrak{D}_{67} = \{(z_1, z_2) : -\phi_1 \le \arg(z_1) \le \phi_1, \arg(z_2) = \phi_2, |z_2| \le x_2\}.$$

From the geometric point of view, the face $\mathcal{F}_{2389}$ separates the dihedral angle region $\mathfrak{D}_{17}$ into two components, one of which, containing the spine of $\mathcal{B}_{17}$, is denoted by $\mathfrak{C}_{17}$. Similarly, we denote by $\mathfrak{C}_{67}$ the component of $\mathfrak{D}_{67}$ separated by $\mathcal{F}_{4589}$ that contains the spine of $\mathcal{B}_{67}$.

Definition 3.23. The side $\mathcal{S}_{17}$ is made up of those points (z_1, z_2) of $\mathcal{B}_{17}$ with

$$-\phi_1 \le \arg(z_1) \le \phi_1, \quad \arg(z_2) = -\phi_2, \quad |z_2| \le x_2,$$

and (z_1, z_2) is lying in $\mathfrak{C}_{17}$.

Definition 3.24. The side $\mathcal{S}_{67}$ is made up of those points (z_1, z_2) of $\mathcal{B}_{67}$ with

$$-\phi_1 \le \arg(z_1) \le \phi_1, \quad \arg(z_2) = \phi_2, \quad |z_2| \le x_2,$$

and (z_1, z_2) is lying in $\mathfrak{C}_{67}$.

3E. ***Sides of wedge type.*** We define, in this section, two special sides $\mathcal{S}_g$ and $\mathcal{S}'_g$ that are not contained in bisectors. These sides are foliated by 2-dimensional cones over arcs of hypercycles contained in Giraud disks.

Projection of the faces $\mathcal{F}_{234}$ and $\mathcal{F}_{345}$. Recall that the orthogonal projection of the face $\mathcal{F}_{234}$ (and $\mathcal{F}_{345}$) onto $\mathcal{C}_1$ is a leaf-shaped region bounded by two arcs of circles, one of which lies inside the face $\mathcal{F}_{789}$ and the other outside; see Figure 5.

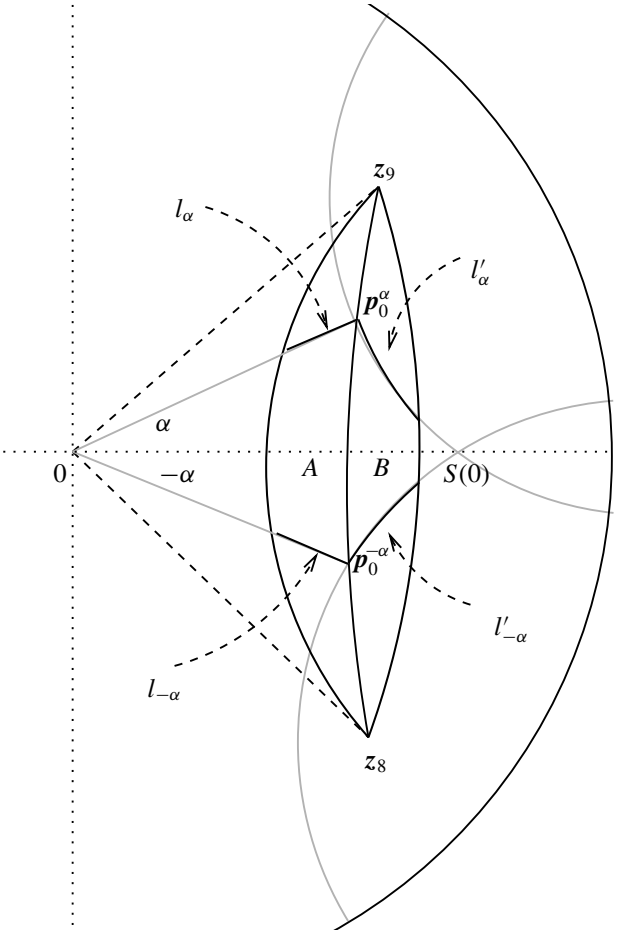

Figure 6. The leaf-shaped region is separated by γ_{89} into A and B. Moreover, A is foliated by l_α for $\alpha \in [-\phi_1, \phi_1]$ and B is foliated by the geodesic arcs l'_α.

The edge γ_{89} separates the leaf-shaped region into two parts, denoted by A and B; see Figure 6.

For $\alpha \in [-\phi_1, \phi_1]$, we denote by l_α the intersection of a straight line with angle α passing through the origin with A. So A is foliated by the straight segments l_α for $\alpha \in [-\phi_1, \phi_1]$. In particular, the straight line segment reduces to a point for $\alpha = \pm\phi_1$ since the preimages of $l_{\pm\phi_1}$ under the orthogonal projection lie in the edge γ_{24} (or γ_{35}). Since the map S restricted to $\mathcal{C}_1$ is of order 2, S swaps A and B. It follows that B is foliated by the geodesic arcs $l'_\alpha = S(l_{-\alpha})$ for $\alpha \in [-\phi_1, \phi_1]$. From Lemma 3.25, we see that l_α and l'_α have the same common endpoint $\boldsymbol{p}_0^\alpha$. Therefore, the connected curves $l_\alpha \cup l'_\alpha$ are leaves of a foliation of the leaf-shaped region $A \cup B$ for $\alpha \in [-\phi_1, \phi_1]$.

Lemma 3.25. *For each* $\alpha \in [-\phi_1, \phi_1]$, $S(\boldsymbol{p}_0^{-\alpha}) = \boldsymbol{p}_0^{\alpha}$.

Proof. Using the z-coordinate in $\mathscr{C}_1$, the edge γ_{89} is a geodesic that can be written as

$$\left| z - \frac{1}{\sqrt{1-4\sin^2\phi_1}} \right| = \frac{2\sin\phi_1}{\sqrt{1-4\sin^2\phi_1}},$$

with $|z| < 1$. Then the point $\boldsymbol{p}_0^{-\alpha} = re^{-i\alpha}$ on the edge γ_{89} satisfies

$$r^2 - \frac{2r\cos\alpha}{\sqrt{1-4\sin^2\phi_1}} + 1 = 0. \tag{3-16}$$

Since S preserves $\mathscr{C}_1$, it suffices to consider the action of S on $\mathscr{C}_1$. Thus (3-16) leads to

$$\begin{aligned} S\big|_{\mathscr{C}_1}(\boldsymbol{p}_0^{-\alpha}) &= \frac{re^{-i\alpha} - \sqrt{1-4\sin^2\phi_1}}{\sqrt{1-4\sin^2\phi_1}re^{-i\alpha} - 1} \\ &= \frac{\sqrt{1-4\sin^2\phi_1}(r^2+1) - 2r\cos\alpha + 4\sin^2\phi_1 re^{i\alpha}}{(1-4\sin^2\phi_1)r^2 - 2r\cos\alpha\sqrt{1-4\sin^2\phi_1} + 1} \\ &= \frac{4\sin^2\phi_1 re^{i\alpha}}{4\sin^2\phi_1} = re^{i\alpha}. \end{aligned}$$

This completes the result. □

Parametrization of the faces $\mathscr{F}_{234}$ *and* $\mathscr{F}_{345}$. We start to parametrize the triangular faces $\mathscr{F}_{234}$ and $\mathscr{F}_{345}$ by the meridian α-parameter.

For convenience, we denote by Π_1 the orthogonal projection onto $\mathscr{C}_1$. Recall that the edge γ_{89} separates the leaf-shaped region into A and B. There exist two curves (denoted by ℓ_{234} and ℓ_{345}) in $\mathscr{F}_{234}$ and $\mathscr{F}_{345}$, respectively, such that $\Pi_1(\ell_{234}) = \Pi_1(\ell_{345}) = \gamma_{89}$; see Figure 7. Furthermore, the curve ℓ_{234} (respectively ℓ_{345}) separates the face $\mathscr{F}_{234}$ (respectively $\mathscr{F}_{345}$) into two parts, one of which is projected to A and the other is projected to B.

For $\alpha \in [-\phi_1, \phi_1]$, we consider the preimage of $l_\alpha \cup l'_\alpha$ on $\mathscr{F}_{234}$, denoted by L^α_{234}. In other words, we have $\Pi_1(L^\alpha_{234}) = l_\alpha \cup l'_\alpha$. Similarly, there is a curve L^α_{345} in $\mathscr{F}_{345}$ such that $\Pi_1(L^\alpha_{345}) = l_\alpha \cup l'_\alpha$. For each $\alpha \in [-\phi_1, \phi_1]$, we see that L^α_{234} and ℓ_{234} (respectively L^α_{345} and ℓ_{345}) intersect in a point whose projection to $\mathscr{C}_1$ is $\boldsymbol{p}_0^\alpha$.

In order to see this, we construct a family of Lagrangian planes that contain the geodesic segments connecting $\boldsymbol{p}_0^\alpha$ and a point of L_{234} (or L_{345}).

(a) Analysis of the preimage $\Pi_1^{-1}(l_\alpha) \subset L^\alpha_{234}$ (the case $\Pi_1^{-1}(l_\alpha) \subset L^\alpha_{345}$ follows similarly): For $s \in [-\lambda, \lambda]$, a slice $\mathscr{C}_s$ of $\mathscr{B}_c$ corresponds to s being constant. We denote by $\boldsymbol{p}_s$ the intersection of the slice $\mathscr{C}_s$ with the edge γ_{16}. The bisector whose spine is the geodesic passing through 0 and $\boldsymbol{p}_s$ in $\mathscr{C}_2$ is denoted by $\mathscr{B}_s$. It follows that $\mathscr{C}_s$ and $\mathscr{C}_1$ are slices of $\mathscr{B}_s$. For a fixed $\alpha \in [-\phi_1, \phi_1]$, some meridian $M_{\alpha,s}$ of

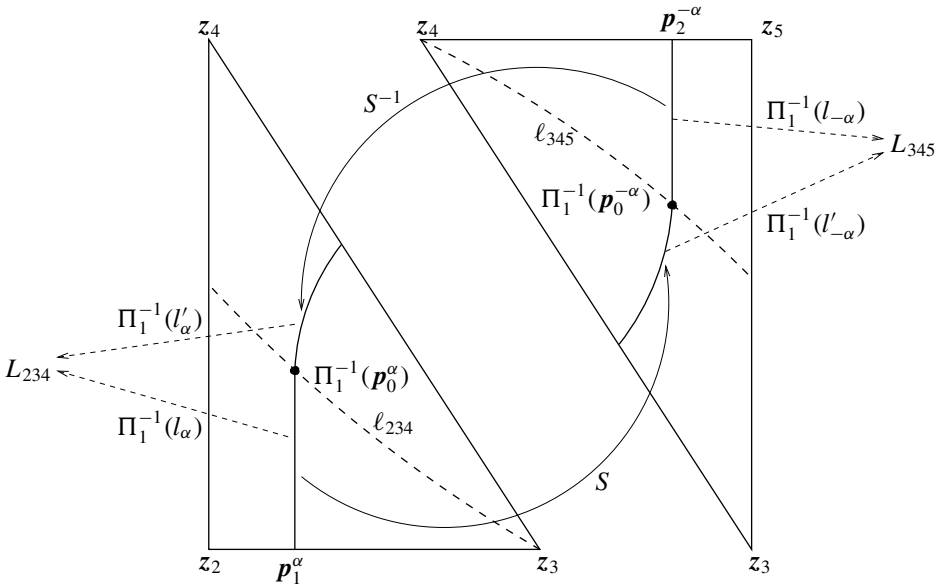

Figure 7. A foliation of the faces $\mathcal{F}_{234}$ (and $\mathcal{F}_{345}$) and the action of S on the leaves of this foliation.

$\mathcal{B}_s$ containing l_α intersects $\mathcal{C}_s$ and $\mathcal{F}_{234}$ in a point (denoted by $\boldsymbol{q}_{\alpha,s}$). For $s = -\lambda$, we see that $\boldsymbol{q}_{\alpha,s} = \boldsymbol{p}_1^\alpha$ and $\Pi_1([\boldsymbol{p}_1^\alpha, \boldsymbol{p}_0^\alpha]) = l_\alpha$. We can take $s_\alpha \in (-\lambda, \lambda)$ such that $\Pi_1([\boldsymbol{q}_{\alpha,s_\alpha}, \boldsymbol{p}_0^\alpha]) = \boldsymbol{p}_0^\alpha$. Thus the locus of points $\boldsymbol{q}_{\alpha,s}$ for $[-\lambda, s_\alpha]$ becomes a curve $\Pi_1^{-1}(l_\alpha) \subset L_{345}^\alpha$; see Figure 7.

(b) Analysis of the preimage $\Pi_1^{-1}(l'_\alpha) \subset L_{234}^\alpha$: We denote by $\boldsymbol{q}'_{-\alpha,s}$ the intersection of $M_{-\alpha,s}$ with $\mathcal{C}_s$ and $\mathcal{F}_{345}$. For a fixed $\alpha \in [-\phi_1, \phi_1]$, we can take $s'_\alpha \in (-\lambda, \lambda)$ such that $\Pi_1([\boldsymbol{q}'_{-\alpha,s'_\alpha}, \boldsymbol{p}_0^{-\alpha}]) = \boldsymbol{p}_0^{-\alpha}$ and $\Pi_1([\boldsymbol{q}'_{-\alpha,\lambda}, \boldsymbol{p}_0^{-\alpha}]) = l_{-\alpha}$. Since the map S preserves $\mathcal{C}_1$, it follows that $\Pi_1(S^{-1}([\boldsymbol{q}'_{-\alpha,s}, \boldsymbol{p}_0^{-\alpha}])) = S^{-1}(\Pi_1([\boldsymbol{q}'_{-\alpha,s}, \boldsymbol{p}_0^{-\alpha}]))$. In particular, we see that

$$\Pi_1(S^{-1}([\boldsymbol{q}'_{-\alpha,s'_\alpha}, \boldsymbol{p}_0^{-\alpha}])) = S^{-1}(\boldsymbol{p}_0^{-\alpha}) = \boldsymbol{p}_0^\alpha,$$
$$\Pi_1(S^{-1}([\boldsymbol{q}'_{-\alpha,\lambda}, \boldsymbol{p}_0^{-\alpha}])) = S^{-1}(l_\alpha) = l'_\alpha.$$

Thus the locus of points $S^{-1}(\boldsymbol{q}'_{-\alpha,s})$ for $[s'_\alpha, \lambda]$ turns out to be a curve, which shares an endpoint with $\Pi_1^{-1}(l_\alpha)$, namely $\boldsymbol{q}_{\alpha,s_\alpha} = S^{-1}(\boldsymbol{q}'_{-\alpha,s'_\alpha})$; see Figure 7. In fact, the geodesic segment $S^{-1}([\boldsymbol{q}'_{-\alpha,s}, \boldsymbol{p}_0^{-\alpha}])$ is contained in the meridian $S^{-1}(M_{-\alpha,s})$ of bisector $S^{-1}(\mathcal{B}_s)$.

The same construction can be implemented for the face $\mathcal{F}_{345}$. This enables us to give the following proposition.

Proposition 3.26. *For each* $\alpha \in [-\phi_1, \phi_1]$, $S(L_{234}^\alpha) = L_{345}^{-\alpha}$.

Sides foliated by 2-dimensional cones. For each $\alpha \in [-\phi_1, \phi_1]$, we define a *sheet* (denoted by $\mathfrak{X}^{\alpha}_{234}$) to be the geodesic cone over L^{α}_{234} to the point $\boldsymbol{p}^{\alpha}_0$. In other words, we join each point of L^{α}_{234} to $\boldsymbol{p}^{\alpha}_0$ by a geodesic segment, that is

$$\mathfrak{X}^{\alpha}_{234} = \bigcup_{z \in L^{\alpha}_{234}} [\boldsymbol{p}^{\alpha}_0, z].$$

Analogously, the sheet $\mathfrak{X}^{\alpha}_{345}$ is defined to be the geodesic cone over L^{α}_{345} to the point $\boldsymbol{p}^{\alpha}_0$, that is

$$\mathfrak{X}^{\alpha}_{345} = \bigcup_{z \in L^{\alpha}_{345}} [\boldsymbol{p}^{\alpha}_0, z].$$

Proposition 3.27. *For $\alpha \neq \beta \in [-\phi_1, \phi_1]$, $\mathfrak{X}^{\alpha}_{234}$ (respectively $\mathfrak{X}^{\alpha}_{345}$) and $\mathfrak{X}^{\beta}_{234}$ (respectively $\mathfrak{X}^{\beta}_{345}$) are disjoint.*

Proof. It suffices to show that the orthogonal projection of $\mathfrak{X}^{\alpha}_{234}$ (or $\mathfrak{X}^{\alpha}_{345}$) onto $\mathscr{C}_1$ is $l_\alpha \cup l'_\alpha$. From Lemma 3.5, the projection of $[z, \boldsymbol{p}^{\alpha}_0]$ is a geodesic segment joining $\boldsymbol{p}^{\alpha}_0$ and $\Pi_1(z)$. Observe that both l_α and l'_α are geodesic segments with common endpoint $\boldsymbol{p}^{\alpha}_0$. For each point z of L^{α}_{234}, it follows that $\Pi_1(z) \in l_\alpha \cup l'_\alpha$, hence $\Pi_1([z, \boldsymbol{p}^{\alpha}_0])$, is contained in $l_\alpha \cup l'_\alpha$. For $\alpha \neq \beta \in [-\phi_1, \phi_1]$, therefore, $\{l_\alpha \cup l'_\alpha\} \cap \{l_\beta \cup l'_\beta\} = \varnothing$ which implies $\mathfrak{X}^{\alpha}_{234} \cap \mathfrak{X}^{\beta}_{234} = \varnothing$ (and $\mathfrak{X}^{\alpha}_{345} \cap \mathfrak{X}^{\beta}_{345} = \varnothing$). □

We are ready to describe the sides $\mathcal{S}_g$ and $\mathcal{S}'_g$; refer to Figure 8 for a schematic view.

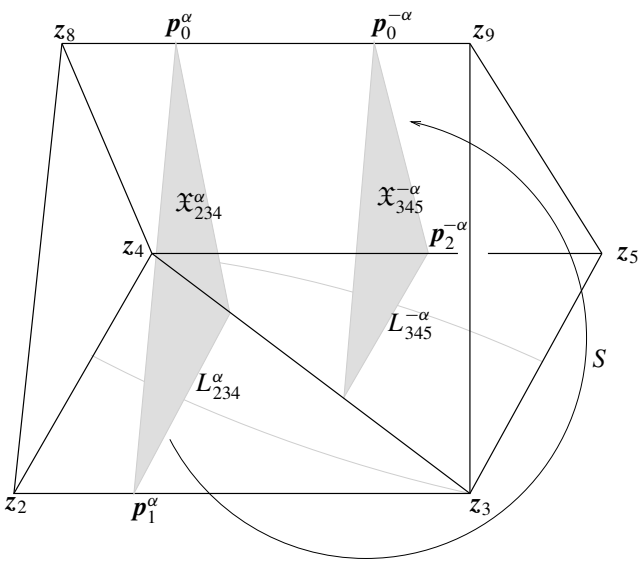

Figure 8. The schematic view of $\mathcal{S}_g$ and $\mathcal{S}'_g$ that are foliated by sheets and the action of S on the sheets.

Definition 3.28. The side S_g is made up of the sheets $\mathfrak{X}^{\alpha}_{234}$ for $\alpha \in [-\phi_1, \phi_1]$, namely, $\mathcal{S}_g = \bigcup_{\alpha\in[-\phi_1,\phi_1]} \mathfrak{X}^{\alpha}_{234}$.

Definition 3.29. The side S'_g is made up of the sheets $\mathfrak{X}^{\alpha}_{345}$ for $\alpha \in [-\phi_1, \phi_1]$, namely, $\mathcal{S}'_g = \bigcup_{\alpha\in[-\phi_1,\phi_1]} \mathfrak{X}^{\alpha}_{345}$.

Remark. The sides $\mathcal{S}_g$ and $\mathcal{S}'_g$ are real differentiable 3-submanifolds. In fact, these sides are foliated by 2-dimensional cones. The cones over arcs of hypercycles are differentiable with respect to the parameter s. It follows from Proposition 3.27 that the sides are unions of disjoint sheets and differentiable with respect to the parameter α.

3F. ***Construction of the polyhedron.*** In the previous sections we constructed eight 3-dimensional cells which are the sides of our polyhedron. In Proposition 3.30 we show that the union of these 3-cells is embedded, so it bounds a topological ball. We now define the polyhedron D to be the interior of the union of the eight sides; see Figure 9. Proposition 3.31 enables us to give a well-defined 4-dimensional domain.

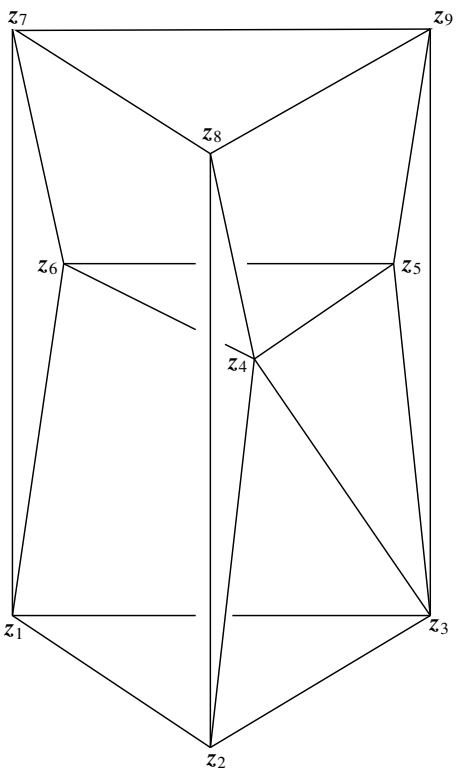

Figure 9. The eight sides of the polyhedron D in complex hyperbolic space (D is the 4-dimensional domain bounded by these sides).

Proposition 3.30. *The union of the eight sides defined in the previous sections is homeomorphic to S^3.*

Proof. Recall the basic geometric fact that S^3 can be interpreted as the union of two 3-balls glued along S^2. We see that, up to homotopy, the core prism $\mathcal{P}_c$ is a 3-ball with boundary $\mathcal{F}_{123} \cup \mathcal{F}_{456} \cup \mathcal{F}_{1246} \cup \mathcal{F}_{1356} \cup \mathcal{F}_{234} \cup \mathcal{F}_{345}$. In Figure 9, it seems that the side $\mathcal{S}_{67}$ lies inside the side $\mathcal{S}_{17}$. However, the sides $\mathcal{S}_{67}$ and $\mathcal{S}_{17}$ share the common face $\mathcal{F}_{789}$ and lie both sides of $\mathcal{F}_{789}$ respectively. It follows that the union of $\mathcal{S}_g$, $\mathcal{S}'_g$, $\mathcal{S}_{17}$, $\mathcal{S}_{67}$, $\mathcal{S}_{78}$ and $\mathcal{S}_{79}$ is a 3-ball whose boundary is also $\mathcal{F}_{123} \cup \mathcal{F}_{456} \cup \mathcal{F}_{1246} \cup \mathcal{F}_{1356} \cup \mathcal{F}_{234} \cup \mathcal{F}_{345}$. This completes the result. □

We also need to ensure that the interior of $\mathcal{S}_g$ and $\mathcal{S}'_g$ cannot intersect the other sides contained in bisectors. This follows directly from the following proposition.

Proposition 3.31. *The interior of $\mathcal{S}_g$ and $\mathcal{S}'_g$ does not intersect the sides contained in bisectors.*

Proof. It suffices to show the interior of each sheet $\mathfrak{X}^{\alpha}_{234}$ (or $\mathfrak{X}^{\alpha}_{345}$) does not meet the sides contained in bisectors for $\alpha \in [-\phi_1, \phi_1]$. We focus on analyzing the sheet $\mathfrak{X}^{\alpha}_{234}$ and the other follows similarly.

Recall that the bisectors containing the sides come in pairs so that the complex spines are the coordinate axes. As in Proposition 1.2.28 of [Thompson 2010], the number of intersection points between a geodesic and a bisector is equal to the number of intersection points between its spine and the projection of the geodesic onto its complex spine. Moreover, it follows from Lemma 3.5 that the projection of a geodesic onto a complex line is an arc of a geometrical circle (and in particular, this is also a geodesic arc if the intersection of the geodesic and the complex line is nonempty). In Lemma 3.6, the projection of a geodesic segment $[z, \boldsymbol{w}]$ onto a coordinate axis is the shorter arc of a geometrical circle with endpoints $\Pi(z)$ and $\Pi(\boldsymbol{w})$ (the images of points under orthogonal projection onto the coordinate axis).

For $\alpha \in [-\phi_1, \phi_1]$ and $z \in L^{\alpha}_{234}$, we consider the projection of the geodesic segment $[\boldsymbol{p}^{\alpha}_0, z]$ onto the coordinate axes $\mathcal{C}_1$ and $\mathcal{C}_2$. For convenience, we also denote by Π_2 the orthogonal projection onto $\mathcal{C}_2$.

(i) The pair of sides $\mathcal{S}_{78}, \mathcal{S}_{79}$ is contained in the bisectors $\mathcal{B}_{78}, \mathcal{B}_{79}$ whose spines contain γ_{78} and γ_{79}. Clearly, $\Pi_1([\boldsymbol{p}^{\alpha}_0, z]) = l_\alpha \cup l'_\alpha$ does not intersect γ_{78} and γ_{79}.

(ii) The pair of sides $\mathcal{S}_{17}, \mathcal{S}_{67}$ is contained in the bisectors $\mathcal{B}_{17}, \mathcal{B}_{67}$ whose spines contain the straight segment γ_{17} and γ_{67}.

• For $z \in \Pi_1^{-1}(l_\alpha)$, the geodesic segment $[\boldsymbol{p}^{\alpha}_0, z]$ is contained in a meridian of $\mathcal{B}_s$. Thus $\Pi_2([\boldsymbol{p}^{\alpha}_0, z])$ is a straight segment with endpoints z_7 and a point of γ_{16} and cannot intersect γ_{17}, γ_{67}.

• For $z \in \Pi_1^{-1}(l'_\alpha)$, we see that $\Pi_1(\mathcal{S}_{17}) = \Pi_1(\mathcal{S}_{67})$ is the geodesic triangular face $\mathcal{F}_{789}$ and $\Pi_1([\boldsymbol{p}^{\alpha}_0, z]) \subset l'_\alpha$. The interior of l'_α does not intersect $\mathcal{F}_{789}$.

(iii) The pair of sides $\mathcal{S}_c, \mathcal{S}'_c$ is contained in the bisector $\mathcal{B}_c$ whose spine contains γ_{16}.

• For $z \in \Pi_1^{-1}(l_\alpha)$, by construction, $\Pi_2([\boldsymbol{p}_0^\alpha, z])$ is a straight segment which intersects γ_{16} only at $\Pi_2(z)$.

• We denote by $(\boldsymbol{p}_0^\alpha, \infty)$ the geodesic extension of $[\boldsymbol{p}_0^\alpha, z]\backslash\{\boldsymbol{p}_0^\alpha\}$ such that z goes to the infinity. For $z \in \Pi_1^{-1}(l'_\alpha)$, observe that $\Pi_1(\boldsymbol{p}_0^\alpha, \infty)$ is a geodesic ray from $\boldsymbol{p}_0^\alpha$ to the boundary passing through $S(0)$; see Figure 6. From the fact that $\Pi_1(\boldsymbol{p}_0^\alpha, \infty)$ does not intersect $\mathcal{F}_{789}$, it follows that $\Pi_2(\boldsymbol{p}_0^\alpha, \infty)$ cannot intersect γ_{17} and γ_{67}. From the geometric view of point, we claim that $\Pi_2([\boldsymbol{p}_0^\alpha, z])$ intersects γ_{16} only at $\Pi_2(z)$. In fact, the interior of $\Pi_2([\boldsymbol{p}_0^\alpha, z])$ can only lie inside the angle region $-\phi_2 \le \arg(z_2) \le \phi_2$. Otherwise, it is not a shorter arc of a circle which is contradiction with Lemma 3.6. Furthermore, if $\Pi_2([\boldsymbol{p}_0^\alpha, z])$ intersects γ_{16} twice, then $\Pi_2(\boldsymbol{p}_0^\alpha, \infty)$ intersects γ_{17} or γ_{67}, which is a contradiction.

From the above analysis, we see that the interior of $[\boldsymbol{p}_0^\alpha, z]$ for $\alpha \in [-\phi_1, \phi_1]$ cannot intersect the sides contained in bisectors. □

4. The main theorem

Our goal is to show that, by Poincaré's polyhedron theorem, the polyhedron D is a fundamental domain and find a presentation, although we already know both that the group Γ_k is discrete and know a presentation of it [Deraux et al. 2005; Parker 2009]. We will prove the following result:

Theorem 4.1. *Suppose that the ordered pair (k, l) is in the list*

$$(7, 42),\ (8, 24),\ (9, 18),\ (10, 15),\ (12, 12),$$
$$(42, 7),\ (24, 8),\ (18, 9),\ (15, 10),$$

that is, $l = 6k/(k-6)$ and k, l are both integers. Then, writing $\phi_1 = \pi/k$ and $\phi_2 = \pi/l$, the group Γ_k generated by the side pairings of D is a discrete subgroup of PU(2, 1) *with fundamental domain D and a presentation*

$$\Gamma_k = \left\langle R, S, T, I_1 \;\middle|\; \begin{array}{ll} T = S^2, & R^k = T^l = (R^{-1}S)^3 = (T^{-1}I_1)^3 \\ R = I_1^2, & \quad = (S^{-1}I_1)^3 = [R, T] = 1 \end{array} \right\rangle. \tag{4-1}$$

Remark. As the roles of k and l are actually symmetric, there are only 5 different groups Γ_k for $k = 7, 8, 9, 10, 12$. Among them only Γ_9 and Γ_{12} are arithmetic, see the table on page 27 of [Parker 2009].

We will prove this theorem by verifying the conditions of the Poincaré's polyhedron theorem, following the strategy outlined below. For the case $k = 6$, that is $l = \infty$, this makes T turn into a parabolic which gives rise to the disappearance

of T^l in the presentation. Thus the group Γ_6 is exactly the same as G_2 (compare [Zhao 2011]), up to conjugation.

Writing $J = S^{-1}I_1$, $R_1 = T^{-1}I_1$, $A_1 = R$ and $A_1' = JTJ^{-1}$, the presentation of Theorem 4.1 becomes

$$\left\langle J, R_1, A_1, A_1' \;\middle|\; \begin{array}{c} J^3 = R_1^3 = A_1^k = {A_1'}^l = 1, \\ A_1 = (JR_1^{-1}J)^2, \quad A_1' = (J^{-1}R_1^{-1}J^{-1})^2, \\ A_1R_1 = R_1A_1, \qquad A_1'R_1 = R_1A_1' \end{array} \right\rangle.$$

Note that $[A_1, R_1] = [R, T]$ follows from $R = I_1^2$ and $[A_1', R_1] = J[T, R]J^{-1}$ follows from

$$T = S^2 \quad \text{and} \quad R^{-1}S = J^{-1}R_1J.$$

This is the presentation in terms of R_1, J given in [Parker 2009] with $p = 3$.

4A. ***Poincaré's polyhedron theorem.*** In this section, we review Poincaré's polyhedron theorem. We will follow the formulation given by Mostow [1980] and also refer to [Deraux et al. 2005; Falbel and Parker 2006; Parker 2009]. We will define a combinatorial polyhedron as a cellular space homeomorphic to a compact polytope, in particular, each of its codimension 2 cells, called *faces*, is contained in exactly two codimension 1 cells, called *sides*. Our polyhedron D is the realization of a combinatorial polyhedron as a cell complex in complex hyperbolic space. A polyhedron is smooth if its cells are smooth. For the boundary of D, the sides contained in bisectors are foliated by a section of slices (or meridians) of bisectors, which are naturally smooth. Nevertheless, the sides that are not contained in bisectors are foliated by geodesic cones with respect to the meridian parameter α, which implies their smoothness. Moreover, the faces foliated by geodesics are also smooth.

Definition 4.2. A *Poincaré polyhedron* is a smooth polyhedron D in a manifold X with sides $\mathcal{S}_j$ and side-pairing maps $g_j \in \operatorname{Isom} X$ satisfying:

(C.1) The sides of the polyhedron are paired by a set Δ of homeomorphisms $g_{ij} : \mathcal{S}_i \longrightarrow \mathcal{S}_j$ of X called the *side-pairing transformations*, which respect the cell structure. We assume that if $g_{ij} \in \Delta$, $g_{ij}^{-1} = g_{ji} \in \Delta$.

(C.2) For every $g_{ij} \in \Delta$ such that $\mathcal{S}_i = g_{ij}(\mathcal{S}_j)$, we have $g_{ij}(\overline{D}) \cap \overline{D} = \mathcal{S}_i$.

Remark. If $\mathcal{S}_i = \mathcal{S}_j$ (that is, a side-pairing maps one side to itself), then we impose the restriction that $g_{ii} : \mathcal{S}_i \longrightarrow \mathcal{S}_i$ is of order two, and we call it a reflection. In this case, the relation $g_{ii}^2 = 1$ is called a reflection relation.

Let $\mathcal{S}_1$ be a side of D and $\mathcal{F}_1$ be a face contained in $\mathcal{S}_1$. Let $\mathcal{S}_1'$ be the other side containing $\mathcal{F}_1$. Let $\mathcal{S}_2$ be the side paired to $\mathcal{S}_1'$ by g_1 and $F_2 = g_1(\mathcal{F}_1)$. Again, there exists only one other side containing $\mathcal{F}_2$, which we call $\mathcal{S}_2'$. We define recursively g_i and $\mathcal{F}_i$, so that $g_{i-1} \circ \cdots \circ g_1(\mathcal{F}_1) = \mathcal{F}_i$.

Definition 4.3. The cyclic condition is that for each pair $(\mathcal{F}_1, \mathcal{S}_1)$ (a face contained in a side), there exists $n \geq 1$ such that, in the construction in the previous paragraph, $g_n \circ \cdots \circ g_1(\mathcal{S}_1) = \mathcal{S}_1$ and $g_n \circ \cdots \circ g_1$ restricted to $\mathcal{F}_1$ is the identity. Moreover, writing $g = g_n \circ \cdots \circ g_1$, there exists a positive integer m such that $g^m = 1$ and

$$g_1^{-1}(D) \cup (g_2 \circ g_1)^{-1}(D) \cup \cdots \cup g^{-1}(D) \cup (g_1 \circ g)^{-1}(D) \cup (g_2 \circ g_1 \circ g)^{-1}(D) \cup \cdots \cup (g^m)^{-1}(D)$$

is a tile of a closed neighborhood of the interior of $\mathcal{F}_1$ by D and its images.

The relation $g^m = (g_n \circ \cdots \circ g_1)^m = \mathrm{Id}$ is called a *cycle relation*.

Remark. We call the positive integer n the *length* of the cycle transformation $g_n \circ g_{n-1} \cdots \circ g_1$ and $n \cdot m$ its total length.

We now state Poincaré's polyhedron theorem:

Theorem 4.4. *Let D be a Poincaré polyhedron with side-pairing transformations $\Delta \subset \mathrm{Isom}\, \boldsymbol{H}^2_{\mathbb{C}}$ in $\boldsymbol{H}^2_{\mathbb{C}}$ satisfying the cyclic condition. Let Γ be the group generated by Δ. Then Γ is a discrete subgroup of $\mathrm{Isom}\, \boldsymbol{H}^2_{\mathbb{C}}$ and D is a fundamental domain of Γ. A presentation of Γ is given by*

$$\Gamma = \langle \Delta \mid \textit{reflection relations}, \textit{cycle relations} \rangle.$$

4B. ***The side pairing maps.*** Let R, T, S and I_1 be given by (2-13), (2-19) and (2-20) respectively. In this section we show that these maps are the side-pairings of our polyhedron D and pair the sides of D as (see Figure 10)

$$R : \mathcal{S}_{78} \longrightarrow \mathcal{S}_{79}, \qquad T : \mathcal{S}_{17} \longrightarrow \mathcal{S}_{67},$$
$$S : \mathcal{S}_g \longrightarrow \mathcal{S}'_g, \qquad I_1 : \mathcal{S}_c \longrightarrow \mathcal{S}'_c.$$

We now verify these maps satisfy conditions (C.1) and (C.2) for each side. By construction, it follows that the side-pairing maps R, S, T satisfy condition (C.1) and we verify the condition (C.1) for the side-pairing map I_1 in Lemma 4.5.

Recall the map I_1 defined in (2-20), and that the action of I_1 on the bisector $\mathcal{B}_c$ (see (3-5)) is given by

$$\frac{e^{-i\phi_1/3}}{2\sin\phi_2} \begin{bmatrix} -2\sin\phi_2 e^{i\phi_1} & 0 & 0 \\ 0 & 1 & -\sqrt{1-4\sin^2\phi_2} \\ 0 & \sqrt{1-4\sin^2\phi_2} & -1 \end{bmatrix} \cdot \begin{bmatrix} \sqrt{1-\mu^2} r e^{i\alpha} \\ \mu + is \\ 1 + i\mu s \end{bmatrix}$$
$$= -e^{-i\phi_1/3} \begin{bmatrix} \sqrt{1-\mu^2} r e^{i(\alpha+\phi_1)} \\ \mu - is \\ 1 - i\mu s \end{bmatrix}.$$

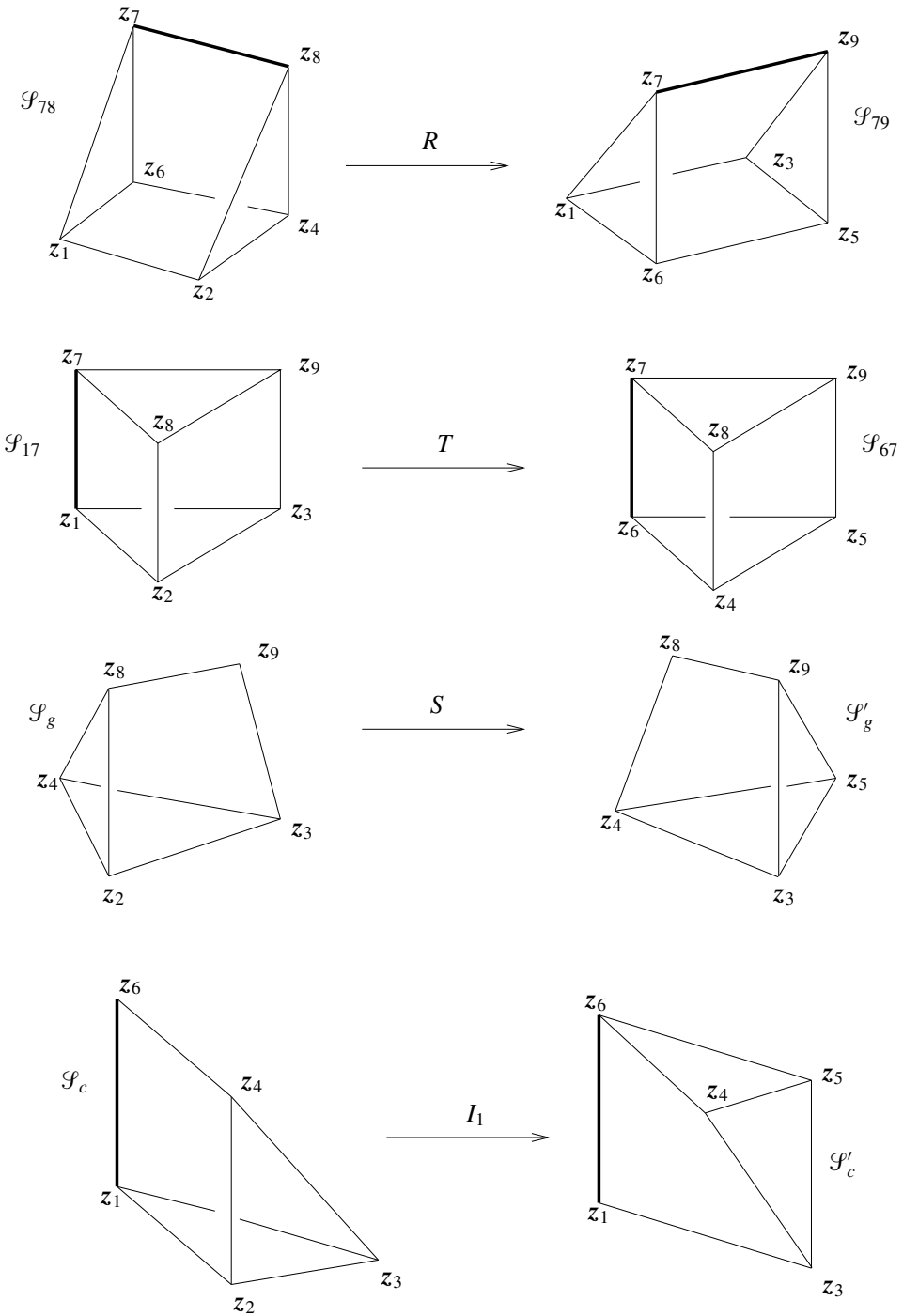

Figure 10. The sides of the polyhedron and the side pairings. The bold lines denote the spines of bisectors.

We see that I_1 maps $\mathcal{B}_c$ to itself, sending the point with coordinates (r, s, α) to the point with coordinates $(r, -s, \alpha + \phi_1)$ when $-\pi/2 \le \alpha < \pi/2 - \phi_1$ or the point with coordinates $(-r, -s, \alpha + \phi_1 - \pi)$ when $\pi/2 - \phi_1 \le \alpha < \pi/2$.

We summarize its action on the vertices of prism by

$$I_1 : \begin{array}{llll} z_1 \longrightarrow z_6, & z_6 \longrightarrow z_1, & & \\ z_2 \longrightarrow z_4, & z_4 \longrightarrow z_3, & z_3 \longrightarrow z_5. & \end{array}$$

Lemma 4.5. $I_1(\mathcal{S}_c) = \mathcal{S}'_c$.

Proof. It suffices to verify the statement for the images of the boundary of $\mathcal{S}_c$ under I_1 since $\mathcal{S}_c, \mathcal{S}'_c$ are contained in $\mathcal{B}_c$ and I_1 preserves the bisector $\mathcal{B}_c$.

• By Lemmas 3.17 and 3.18, we see easily that

$$I_1(\gamma_{16}) = \gamma_{16}, \quad I_1(\gamma_{12}) = \gamma_{46}, \quad I_1(\gamma_{13}) = \gamma_{56}, \quad I_1(\gamma_{24}) = \gamma_{34}, \quad I_1(\gamma_{34}) = \gamma_{35},$$

which implies $I_1(\mathcal{F}_{1246}) = \mathcal{F}_{1346}$ and $I_1(\mathcal{F}_{1346}) = \mathcal{F}_{1356}$ by construction.

• The face $\mathcal{F}_{234}$ is contained in the intersection $\mathcal{B}_c \cap S^{-1}(\mathcal{B}_c) = \mathcal{B}_c \cap J(\mathcal{B}_c)$, which is a Giraud disk. We have

$$J(\mathcal{F}_{234}) \subset J(\mathcal{B}_c) \cap J^{-1}(\mathcal{B}_c) \quad \text{and} \quad J^{-1}(\mathcal{F}_{234}) \subset J^{-1}(\mathcal{B}_c) \cap \mathcal{B}_c$$

since J is a regular elliptic element of order 3. As J permutes the edges γ_{23}, γ_{34} and γ_{24}, the triple intersection $\mathcal{B}_c \cap J(\mathcal{B}_c) \cap J^{-1}(\mathcal{B}_c)$ contains γ_{23}, γ_{34} and γ_{24}. It follows from Proposition 3.4 that $J^{-1}(\mathcal{B}_c) = I_1^{-1} S(\mathcal{B}_c)$ is the third bisector containing the face $\mathcal{F}_{234}$. Obviously, the map I_1 sends points of $\mathcal{B}_c \cap I_1^{-1} S(\mathcal{B}_c)$ to points of $\mathcal{B}_c \cap S(\mathcal{B}_c)$. Furthermore, the edge γ_{23} is contained in $\mathcal{B}_c \cap I_1^{-1} S(\mathcal{B}_c)$ with $s_0 = -\lambda$ and the edge γ_{45} is contained in $\mathcal{B}_c \cap S(\mathcal{B}_c)$ with $s_0 = \lambda$, which implies that $I_1(\gamma_{23}) = \gamma_{45}$. From the above argument, we obtain $I_1(\mathcal{F}_{234}) = \mathcal{F}_{345}$ and $I_1(\mathcal{F}_{123}) = \mathcal{F}_{456}$. □

We give the following lemma to verify condition (C.2) for each side.

Lemma 4.6. *If g is one of R, S, T, I_1, then $g^{-1}(D) \cap D = g(D) \cap D = \varnothing$. Also,*

$$R^{-1}(\overline{D}) \cap \overline{D} = \mathcal{S}_{78}, \; T^{-1}(\overline{D}) \cap \overline{D} = \mathcal{S}_{17}, \; S^{-1}(\overline{D}) \cap \overline{D} = \mathcal{S}_g, \; I_1^{-1}(\overline{D}) \cap \overline{D} = \mathcal{S}_c,$$
$$R(\overline{D}) \cap \overline{D} = \mathcal{S}_{79}, \quad T(\overline{D}) \cap \overline{D} = \mathcal{S}_{67}, \quad S(\overline{D}) \cap \overline{D} = \mathcal{S}'_g, \quad I_1(\overline{D}) \cap \overline{D} = \mathcal{S}'_c.$$

Proof. We divide into three cases:

(i) Consider the side $\mathcal{S}_{78}$ (the sides $\mathcal{S}_{79}, \mathcal{S}_{17}, \mathcal{S}_{67}$ follow similarly). If $z \in \overline{D}$ then $-\phi_1 \le \arg(z_1) \le \phi_1$ with equality only when $z \in \mathcal{B}_{78}$ (or $\mathcal{B}_{79}$). Likewise, if $w = R(z) \in \overline{D}$ then $-\phi_1 \le \arg(e^{i2\phi_1} z_1) \le \phi_1$. Hence if $R(z) \in \overline{D}$, or equivalently $z \in R^{-1}(D)$, then $-3\phi_1 \le \arg(z_1) \le -\phi_1$. Thus $z \in \overline{D} \cap R^{-1}(\overline{D})$ if and only if $z \in \mathcal{B}_{78}$ and precisely $z \in \mathcal{S}_{78}$.

(ii) Consider the core sides $\mathcal{S}_c$ and $\mathcal{S}'_c$. Observe that I_1 preserves $\mathcal{B}_c$ and swaps one side of $\mathcal{B}_c$ with the other. If $z = (z_1, z_2) \in \overline{D}$ then

$$2\sin\phi_2|z_2| \le \left|z_2 - \sqrt{1-4\sin^2\phi_2}\,\right|$$

with equality only when $z \in \mathcal{S}_c \cup \mathcal{S}'_c$. If $z \in D$, then $w = I_1(z)$ satisfying

$$2\sin\phi_2|w_2| > \left|w_2 - \sqrt{1-4\sin^2\phi_2}\,\right|$$

does not intersect $\overline{D}$. Only $z \in \mathcal{S}_c$ (respectively $z \in \mathcal{S}'_c$) satisfy $I_1(z) \in \mathcal{S}'_c$ (respectively $I_1^{-1}(z) \in \mathcal{S}_c$).

(iii) Consider the sides $\mathcal{S}_g$ and $\mathcal{S}'_g$. By construction, we see that $S(\mathcal{S}_g) = \mathcal{S}'_g$. It suffices to show that S-images of the sides (except for $\mathcal{S}_g$) do not intersect the sides of D.

• The pair $S(\mathcal{S}_{78})$ and $S(\mathcal{S}_{79})$: Observe that the spine of $S(\mathcal{S}_{78})$ (or $S(\mathcal{S}_{79})$) is the geodesic segment between $S(0)$ and z_8 (or z_9) in $\mathcal{C}_1$. It follows easily from their projections in $\mathcal{C}_1$ that there is no intersection of the interior of $S(\mathcal{S}_{78})$ (or $S(\mathcal{S}_{79})$) with the sides of D.

• The pair $S(\mathcal{S}_{17})$ and $S(\mathcal{S}_{67})$: The fact that the map S preserves $\mathcal{C}_1$ implies $\Pi_1(S(\mathcal{S}_{17})) = S(\Pi_1(\mathcal{S}_{17}))$ and $\Pi_1(S(\mathcal{S}_{67})) = S(\Pi_1(\mathcal{S}_{67}))$, that is, it preserves the geodesic triangle with vertices $z_8, z_9, S(0)$ in $\mathcal{C}_1$. It follows that the pair doesn't intersect the sides $\mathcal{S}_{78}$ and $\mathcal{S}_{79}$. Observe that the complex spine of $S(\mathcal{S}_{17})$ (or $S(\mathcal{S}_{67})$) turns into $S(\mathcal{C}_2)$, that is, the complex line $z_1 = \sqrt{1-4\sin^2\phi_1}$. Since the map S restricted to $\mathcal{C}_2$ is a Möbius transformation, the spine of $S(\mathcal{S}_{17})$ (or $S(\mathcal{S}_{67})$) is the straight line segment between $S(0)$ and $S(z_1)$ (or $S(z_6)$). From the fact that both $S(\mathcal{C}_2)$ and $\mathcal{C}_2$ are orthogonal to $\mathcal{C}_1$, we see that the projection of $S(\mathcal{S}_{17})$ (or $S(\mathcal{S}_{67})$) is the same as the projection of its spine onto $\mathcal{C}_2$. It follows from $S(z_1) = 2\sin\phi_1 x_2 < \mu$ and $S(z_6) = 2\sin\phi_1 x_2 e^{2i\phi_2}$ that the interior of projection of the spines of $S(\mathcal{S}_{17})$ and $S(\mathcal{S}_{67})$ lie inside or outside the geodesic triangle $\mathcal{F}_{167}$. Therefore, they don't intersect $\mathcal{S}_{17}, \mathcal{S}_{67}, \mathcal{S}_c$ and $\mathcal{S}'_c$. Finally, it follows from Proposition 3.31 that $\mathcal{S}_{67} \cap \mathcal{S}'_g = \varnothing$ and $\mathcal{S}_{17} \cap \mathcal{S}_g = \varnothing$, which implies that $S(\mathcal{S}_{17})$ does not intersect $\mathcal{S}_g$ and $\mathcal{S}'_g$. The side $S(\mathcal{S}_{67})$ follows similarly.

• The pair $S(\mathcal{S}_c)$, $S(\mathcal{S}'_c)$ and the side $S(\mathcal{S}'_g)$: It follows from Definitions 3.19 and 3.20 that $S(\mathcal{S}_c)$ and $S(\mathcal{S}'_c)$ don't intersect $\mathcal{S}_c$) and $\mathcal{S}'_c$. Moreover, the same argument by replacing S by S^{-1} as above implies that $S(\mathcal{S}_c)$ and $S(\mathcal{S}'_c)$ don't intersect other sides. In the end, we see that $S(\mathcal{S}'_g) = T(\mathcal{S}_g)$ and $T(\overline{D}) \cap \overline{D} = \mathcal{S}_{67}$. Therefore, $T(\mathcal{S}_g) \cap \mathcal{S}_{67} = \varnothing$ implies that the side $S(\mathcal{S}'_g)$ does not intersect $\overline{D}$. □

4C. ***The face cycles.*** We now write the face cycles induced by the side-pairings in terms of type of face, and the label of each face reflects the order of vertices.

• $\mathbb{C}$-planar triangle cycles:

$$\mathscr{F}_{167} \xrightarrow{R} \mathscr{F}_{167}, \qquad \mathscr{F}_{123} \xrightarrow{I_1} \mathscr{F}_{645} \xrightarrow{T^{-1}} \mathscr{F}_{123},$$
$$\mathscr{F}_{789} \xrightarrow{T} \mathscr{F}_{789}, \qquad \mathscr{F}_{248} \xrightarrow{S} \mathscr{F}_{359} \xrightarrow{R^{-1}} \mathscr{F}_{248}.$$

• $\mathbb{R}$-planar quadrilateral cycles:

$$\mathscr{F}_{1287} \xrightarrow{T} \mathscr{F}_{6487} \xrightarrow{R} \mathscr{F}_{6597} \xrightarrow{T^{-1}} \mathscr{F}_{1397} \xrightarrow{R^{-1}} \mathscr{F}_{1287}.$$

• Giraud triangle cycles:

$$\mathscr{F}_{234} \xrightarrow{I_1} \mathscr{F}_{453} \xrightarrow{S^{-1}} \mathscr{F}_{342} \xrightarrow{I_1} \mathscr{F}_{534} \xrightarrow{S^{-1}} \mathscr{F}_{423} \xrightarrow{I_1} \mathscr{F}_{345} \xrightarrow{S^{-1}} \mathscr{F}_{234}.$$

• Generic quadrilateral cycles:

$$\mathscr{F}_{1246} \xrightarrow{I_1} \mathscr{F}_{6431} \xrightarrow{I_1} \mathscr{F}_{1356} \xrightarrow{R^{-1}} \mathscr{F}_{1246},$$
$$\mathscr{F}_{2398} \xrightarrow{S} \mathscr{F}_{3489} \xrightarrow{S} \mathscr{F}_{4598} \xrightarrow{T^{-1}} \mathscr{F}_{2398}.$$

4D. ***Verifying the tessellation conditions.*** In this section we verify the cyclic condition of the Poincaré's polyhedron theorem; we refer to [Deraux et al. 2005] and [Parker 2006] for more details. Recall that for a face cycle,

$$\mathscr{F}_1 \xrightarrow{g_1} \mathscr{F}_2 \xrightarrow{g_2} \cdots \longrightarrow \mathscr{F}_n \xrightarrow{g_n} \mathscr{F}_1.$$

The cycle transformation $g_n \circ g_{n-1} \circ \cdots \circ g_1$ acts on $\mathscr{F}_1$ as the identity and there is a certain integer m such that $(g_n \circ g_{n-1} \circ \cdots \circ g_1)^m = \mathrm{Id}$. In order to verify the cyclic condition we must show that there is a neighborhood U of the interior of the face such that U is tiled by $\overline{D}$ and its images under relevant side pairings. Specifically, for the above face cycle, the images $g_1^{-1}(D)$, $(g_2 \circ g_1)^{-1}(D)$, …, $((g_n \circ g_{n-1} \circ \cdots \circ g_1)^m)^{-1}(D) = D$ of D tessellate a neighborhood of $\mathscr{F}_1$. It suffices to consider a neighborhood U of one member of a given face cycle since the others are images of U under suitable side-pairings.

Tessellation around $\mathbb{C}$-planar faces. In this section we consider the faces contained in a complex line. These are the faces $\mathscr{F}_{123}$, $\mathscr{F}_{456}$, $\mathscr{F}_{789}$, $\mathscr{F}_{167}$, $\mathscr{F}_{248}$ and $\mathscr{F}_{359}$. They form four face cycles described again as

$$\mathscr{F}_{167} \xrightarrow{R} \mathscr{F}_{167} \quad \text{and} \quad \mathscr{F}_{789} \xrightarrow{T} \mathscr{F}_{789}.$$

The face $\mathscr{F}_{167}$ is contained in the intersection of two bisectors $\mathscr{B}_{78}$ and $\mathscr{B}_{79}$. If a point $z = (z_1, z_2) \in \overline{D}$, then $-\phi_1 \le \arg(z_1) \le \phi_1$ and the face $\mathscr{F}_{167}$ is contained in $z_1 = 0$. We know R acts on the z_1-plane as a rotation with angle $2\phi_1$. Therefore, the union of the images of $\overline{D}$ under R^i for $i = 1, 2, \ldots, k$ covers a neighborhood of the face $\mathscr{F}_{167}$. Similarly, the union of the images of $\overline{D}$ under T^j for $j = 1, 2, \ldots, l$

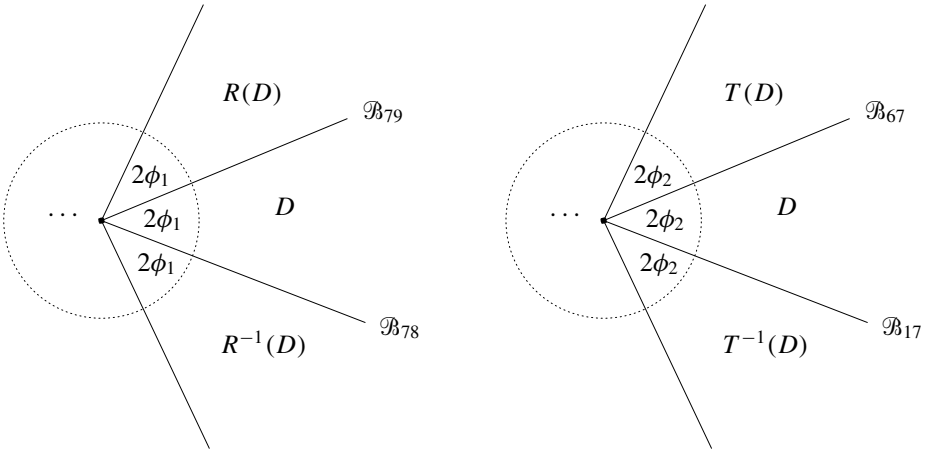

Figure 11. Left: Images of $\overline{D}$ under powers of R tiling a neighborhood of the face $\mathcal{F}_{167}$. Right: Images of $\overline{D}$ under powers of T tiling a neighborhood of the face $\mathcal{F}_{789}$.

covers a neighborhood of the face $\mathcal{F}_{789}$; refer to Figure 11 for a schematic view of their images. If the group is discrete, these elliptic elements must have finite order which implies that k, l must be integers. Together with the condition $1/k+1/l=\frac{1}{6}$, we obtain the pairs (k, l) listed in Theorem 4.1. Otherwise the group is not discrete [Mostow 1988]. From the geometric point of view, in nondiscrete cases, D may intersect its image under some nontrivial power of R or T.

Proposition 4.7. *The polyhedron D and its images under powers of R (respectively T) tessellate around the face $\mathcal{F}_{167}$ (respectively $\mathcal{F}_{789}$). The cycle transformation corresponding to the face $\mathcal{F}_{167}$ (respectively $\mathcal{F}_{789}$) is R (respectively T) and $n=1, m=k$ (respectively $m=l$). This gives the cycle relation $R^k=T^l=1$.*

The remaining two face cycles are

$$\mathcal{F}_{123} \xrightarrow{I_1} \mathcal{F}_{456} \xrightarrow{T^{-1}} \mathcal{F}_{123} \quad \text{and} \quad \mathcal{F}_{248} \xrightarrow{S} \mathcal{F}_{359} \xrightarrow{R^{-1}} \mathcal{F}_{248}.$$

Both $T^{-1}I_1$ and $R^{-1}S$ are complex reflections. The main difference between them is that the face $\mathcal{F}_{123}$ is in the intersection of two bisectors $\mathcal{B}_c, \mathcal{B}_{17}$ and the face $\mathcal{F}_{248}$ is in the intersection of the bisector $\mathcal{B}_{78}$ with the side S_g, which is not contained in a bisector. The schematic 2-dimensional pictures of coverings of neighborhoods of $\mathcal{F}_{123}$ and $\mathcal{F}_{248}$ are the same; see Figure 12.

Proposition 4.8. *The polyhedron D and its images under I_1^{-1}, $I_1^{-1}T$, $I_1^{-1}TI_1^{-1}$, $T^{-1}I_1$ and T^{-1} tessellate around the face $\mathcal{F}_{123}$. The cycle transformation corresponding to the face $\mathcal{F}_{123}$ is $T^{-1}I_1$ and $n=2, m=3$. This gives the cycle relation $(T^{-1}I_1)^3=1$.*

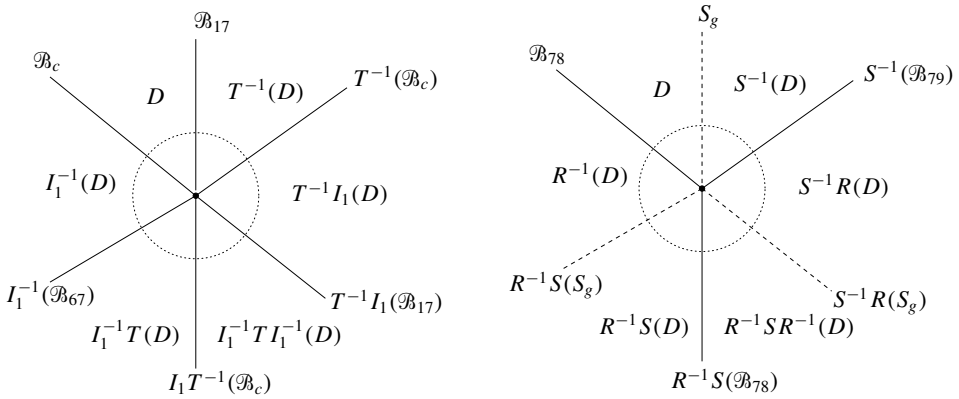

Figure 12. Left: Images of $\overline{D}$ covering a neighborhood of the face $\mathcal{F}_{123}$. Right: Images of $\overline{D}$ covering a neighborhood of the face $\mathcal{F}_{248}$. The black points at the center indicate the corresponding faces.

Proposition 4.9. *The polyhedron D and its images under R^{-1}, $R^{-1}S$, $R^{-1}SR^{-1}$, $S^{-1}R$ and S^{-1} tessellate around the face $\mathcal{F}_{248}$. The cycle transformation corresponding to the face $\mathcal{F}_{248}$ is $R^{-1}S$ and $n=2$, $m=3$. This gives the cycle relation $(R^{-1}S)^3=1$.*

Tessellation around $\mathbb{R}$-planar faces. In this section we only consider a single face cycle in which the faces are all contained in Lagrangian planes. The associate face cycle is

$$\mathcal{F}_{1278} \xrightarrow{T} \mathcal{F}_{4678} \xrightarrow{R} \mathcal{F}_{5679} \xrightarrow{T^{-1}} \mathcal{F}_{1379} \xrightarrow{R^{-1}} \mathcal{F}_{1278}.$$

The schematic image of the tiling of a neighborhood of the face $\mathcal{F}_{1278}$ is

$$\begin{array}{c|c} D & R^{-1}(D) \\ \hline T^{-1}(D) & T^{-1}R^{-1}(D). \end{array}$$

The fact that D and its images as above have disjoint interiors follows easily from Lemma 4.6. Moreover, the bisector $\mathcal{B}_{17}$ separates D and $T^{-1}(D)$, the bisector $\mathcal{B}_{78}$ separates D and $R^{-1}(D)$. Thus applying T^{-1} to D and $R^{-1}(D)$, we see that the bisector $T^{-1}(\mathcal{B}_{78})$ separates $T^{-1}(D)$ and $T^{-1}R^{-1}(D)$. Analogously, applying R^{-1} to D and $T^{-1}(D)$, the bisector $R^{-1}(\mathcal{B}_{17})$ separates $R^{-1}(D)$ and $R^{-1}T^{-1}(D)=T^{-1}R^{-1}(D)$.

Proposition 4.10. *The polyhedron D and its images under T^{-1}, R^{-1} and $T^{-1}R^{-1}$ tessellate around the face $\mathcal{F}_{1278}$. The cycle transformation corresponding to the face $\mathcal{F}_{1278}$ is $R^{-1}T^{-1}RT$ and $n=4$, $m=1$. This gives the cycle relation $[T,R]=1$.*

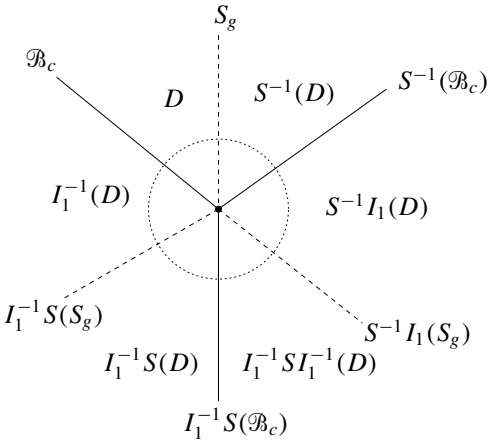

Figure 13. The images of $\overline{D}$ covering a neighborhood of the face $\mathcal{F}_{234}$. The black point at the center indicates the face $\mathcal{F}_{234}$.

Tessellation around the face $\mathcal{F}_{234}$. The face $\mathcal{F}_{234}$ is contained in a Giraud disk that is the intersection of $\mathcal{B}_c$, $S^{-1}(\mathcal{B}_c)$ and $I_1^{-1}S(\mathcal{B}_c)$. It is given by an equation of the form

$$|\langle z, \boldsymbol{n}_0\rangle| = |\langle z, I_1^{-1}(\boldsymbol{n}_0)\rangle| = |\langle z, I_1^{-1}SI_1^{-1}(\boldsymbol{n}_0)\rangle|.$$

As in the arguments in Section 7.8 of [Falbel et al. 2011], we see that there are three regions where the first (respectively second and third) of these quantities as above is the smallest tessellate around the face $\mathcal{F}_{234}$. Observe that the points of D around the face $\mathcal{F}_{234}$ locally lie in the corner bounded by $\mathcal{B}_c$ and $\mathcal{S}_g$. Similarly the points of $S^{-1}(D)$ around $\mathcal{F}_{234}$ locally lie in the corner bounded by $S^{-1}(\mathcal{B}_c)$ and the side $\mathcal{S}_g$. Thus the union of D and $S^{-1}(D)$ covers a neighborhood of $\mathcal{F}_{234}$ in the region where the first quantity is smallest. Applying the elements $S^{-1}I_1$ and $I_1^{-1}S$, we see that the images $I_1^{-1}(D)$, $I_1^{-1}S(D)$, $I_1^{-1}SI_1^{-1}(D)$ and $S^{-1}I_1(D)$ cover the other two regions; see Figure 13. There is a difference around the faces $\mathcal{F}_{123}$ (or $\mathcal{F}_{248}$) and $\mathcal{F}_{234}$, that is not apparent from the 2-dimensional picture. We give the difference in the following proposition.

Proposition 4.11. *The polyhedron D and its images under I_1^{-1}, $I_1^{-1}S$, $I_1^{-1}SI_1^{-1}$, $S^{-1}I_1$ and S^{-1} tessellate around the face $\mathcal{F}_{234}$. The cycle transformation corresponding to the face $\mathcal{F}_{234}$ is $(S^{-1}I_1)^3$ and $n = 6$, $m = 1$. This gives the cycle relation $(S^{-1}I_1)^3 = 1$.*

Tessellation around the generic quadrilateral faces. In this section we consider the faces of D that are neither contained in a complex line nor in a Lagrangian plane nor in a Giraud disk. These faces are foliated by geodesics.

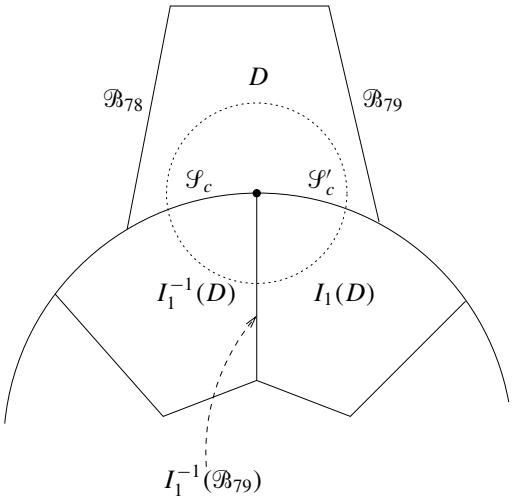

Figure 14. Images of $\overline{D}$ covering a neighborhood of the face $\mathcal{F}_{1346}$. The black point at the center indicates the face $\mathcal{F}_{1346}$.

We first consider the face $\mathcal{F}_{1346}$, the associated face cycle is

$$\mathcal{F}_{1346} \xrightarrow{I_1} \mathcal{F}_{1356} \xrightarrow{R^{-1}} \mathcal{F}_{1246} \xrightarrow{I_1} \mathcal{F}_{1346}.$$

This is the same situation as in [Zhao 2011].

Observe that $\mathcal{F}_{1346}$ is the common face of $\mathcal{S}_c$ and $\mathcal{S}'_c$ contained in $\mathcal{B}_c$. As it is known that a bisector separates complex hyperbolic space into two components, we say D covers the part of a neighborhood of $\mathcal{F}_{1346}$ in the component of $\boldsymbol{H}^2_{\mathbb{C}}\backslash\mathcal{B}_c$ defined by $\{z \in \boldsymbol{H}^2_{\mathbb{C}} : |\langle z, \boldsymbol{n}_0\rangle| < |\langle z, I_1^{-1}(\boldsymbol{n}_0)\rangle|\}$; refer to Figure 14 for the 2-dimensional view. Observe that I_1 swaps one component of $\mathcal{B}_c$ with the other. Also, $I_1^{-1}(\overline{D})\cap\overline{D} = \mathcal{S}_c$, $I_1(\overline{D})\cap\overline{D} = \mathcal{S}'_c$ and $I_1^{-1}(\overline{D})\cap I_1(\overline{D}) = I_1^{-1}(\mathcal{S}_{79}) = I_1(\mathcal{S}_{78})$. Therefore $\overline{D}\cup I_1^{-1}(\overline{D})\cup I_1(\overline{D})$ covers a neighborhood of $\mathcal{F}_{1346}$.

Proposition 4.12. *The polyhedron D and its images under I_1^{-1} and I_1 tessellate around the face $\mathcal{F}_{1346}$. The cycle transformation corresponding to the face $\mathcal{F}_{1346}$ is $I_1R^{-1}I_1$ and $n = 3, m = 1$. This gives the cycle relation $I_1R^{-1}I_1 = 1$.*

For the face $\mathcal{F}_{3489}$, the associated face cycle is

$$\mathcal{F}_{3489} \xrightarrow{S} \mathcal{F}_{4589} \xrightarrow{T^{-1}} \mathcal{F}_{2389} \xrightarrow{S} \mathcal{F}_{3489}.$$

The face $\mathcal{F}_{3489}$ is the intersection of $\mathcal{S}_g$ and $\mathcal{S}'_g$. The union $\mathcal{S}_g \cup \mathcal{S}'_g$ locally separates $\boldsymbol{H}^2_{\mathbb{C}}$ into two components, one of which is contained in D. Since the map S restricted to $\mathcal{C}_1$ is of order 2, the image $S(D)$ (or $S^{-1}(D)$) is contained in the

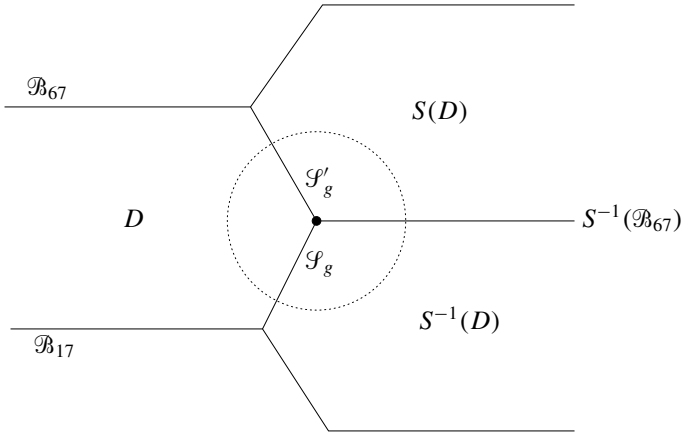

Figure 15. Images of $\overline{D}$ covering a neighborhood of the face $\mathcal{F}_{3489}$. The black point at the center indicates the face $\mathcal{F}_{3489}$.

other component; see Figure 15. In fact, $S^{-1}(\overline{D}) \cap \overline{D} = \mathcal{S}_g$ and $S(\overline{D}) \cap \overline{D} = \mathcal{S}'_g$ by Lemma 4.6. It is obvious that $S^{-1}(\overline{D}) \cap S(\overline{D}) = S^{-1}(\mathcal{S}_{67}) = S(\mathcal{S}_{17})$ is contained in a bisector, and $\mathcal{S}_g \cap \mathcal{S}'_g \cap S^{-1}(\mathcal{S}_{67}) = \mathcal{F}_{1346}$. The result follows from the same argument as above.

Proposition 4.13. *The polyhedron D and its images under S^{-1} and S tessellate around the face $\mathcal{F}_{3489}$. The cycle transformation corresponding to the face $\mathcal{F}_{3489}$ is $ST^{-1}S$ and $n = 3$, $m = 1$. This gives the cycle relation $ST^{-1}S = 1$.*

This completes the proof of Theorem 4.1 by the Poincaré polyhedron theorem with Propositions 4.7–4.13.

5. Mostow groups of the second type

We review, in this section, the Mostow groups of the second type. Our review is based on related materials in [Parker 2009]. It aims to explain briefly how the previous construction of fundamental domains might be adapted for all Mostow groups of the second type.

Let $\Gamma(p, k)$ denote the equilateral triangle group $\langle R_1, R_2, R_3 \rangle$ where each R_i is of order p. Mostow groups of the second type are the groups $\Gamma(p, k)$ where the values of p, k and $l = 1/(1/2 - 1/p - 1/k)$ are given as follows, where the values of k and l can be interchanged.

p	3	3	3	3	3	4	4	4	5	5	6	6
k	7	8	9	10	12	5	6	8	5	5	4	6
l	42	24	18	15	12	20	12	8	20	10	12	6

We begin with the given geometrical generators (as defined in Section 2A), $R = (JR_1^{-1}J)^2$, $S = JR_1^{-1}$, $T = (JR_1^{-1})^2$, $I_1 = JR_1^{-1}J$. From (5.3) of [Parker 2009] and the above setting, we obtain the presentation

$$\text{(5-1)}\quad \Gamma(p,k) = \left\langle R, S, T, I_1 \;\middle|\; \begin{array}{ll} T = S^2, & R^k = T^l = (R^{-1}S)^p = (T^{-1}I_1)^p \\ R = I_1^2, & = (S^{-1}I_1)^3 = [R,T] = 1 \end{array} \right\rangle.$$

This enables us to give the inspiration of the construction of the same shape of combinatorial polyhedra as in the previous sections.

The key point of construction is to analyze whether the group $\langle R, S, T\rangle$ is the stabilizer fixing a point in the interior (or in the boundary) or a complex line. As we computed in § 2.2, the common eigenvector of R and S is

$$\boldsymbol{n} = \begin{bmatrix} u^2\overline{\tau} & \overline{u}^2\tau & -1 \end{bmatrix}^t.$$

By an easy calculation, we obtain

$$\begin{aligned} \langle \boldsymbol{n}, \boldsymbol{n}\rangle_H &= \begin{bmatrix} \overline{u}^2\tau & u^2\overline{\tau} & -1 \end{bmatrix} H \begin{bmatrix} u^2\overline{\tau} \\ \overline{u}^2\tau \\ -1 \end{bmatrix} \\ &= 1 - u^3 + \overline{u}^6\tau^3 - \overline{u}^3\tau^3 + u^6\overline{\tau}^3 - u^3\overline{\tau}^3 + 1 - \overline{u}^3 \\ &= 2\left[1 - \cos\tfrac{2\pi}{p} - \cos\left(\tfrac{4\pi}{p} + \tfrac{2\pi}{k}\right) + \cos\left(\tfrac{2\pi}{p} + \tfrac{2\pi}{k}\right)\right] \\ &\triangleq 2N(p,k). \end{aligned}$$

The basic construction requires that the stabilizer fixe a complex line. It suffices to analyze the norm of $\boldsymbol{n}$ and obtain the positive norm as required.

(i) For $p = 4$,

$$N(4,k) = 1 - \sqrt{2}\sin\left(\tfrac{2\pi}{k} - \tfrac{\pi}{4}\right),$$

then $N(4,k) \geq 0$ if and only $k \geq 4$.

(ii) For $p = 5$,

$$N(5,k) = 1 - \cos\tfrac{2\pi}{5} + 2\sin\left(\tfrac{3\pi}{5} + \tfrac{2\pi}{k}\right)\sin\tfrac{\pi}{5} > 0.$$

(iii) For $p = 6$,

$$N(6,k) = \tfrac{1}{2} + \cos\tfrac{2\pi}{k}.$$

then $N(6,k) \geq 0$ if and only $k \geq 3$.

As a matrix of $\mathrm{SU}(H)$,

$$T = \begin{bmatrix} 0 & \overline{u}^2 & 0 \\ -\overline{u}^3\tau & \overline{u}^2\tau^2 + u\overline{\tau} & 0 \\ \overline{u} & -\tau & u\overline{\tau} \end{bmatrix},$$

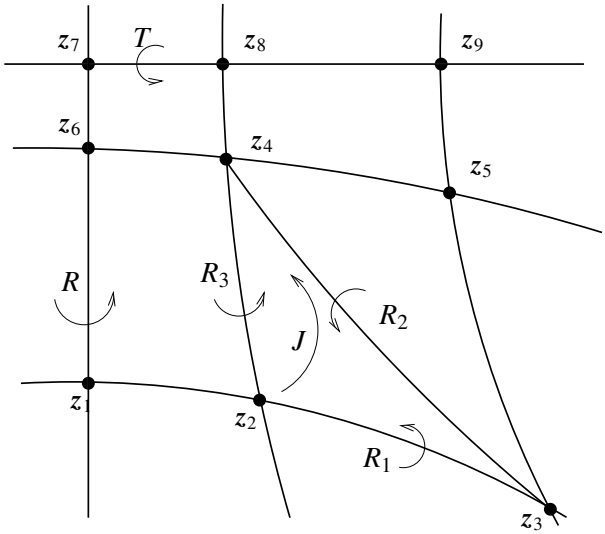

Figure 16. The construction in two dimensions: the lines indicated are complex and the vertices of polyhedron arise from the intersections of two complex lines.

so T has the eigenvalue $\overline{u}^2\tau^2$ corresponding to $\boldsymbol{n}$ and a repeated eigenvalue $u\overline{\tau}$. Hence the relation $T^l = 1$ implies that

$$1/l = 1/2 - 1/p - 1/k \tag{5-2}$$

Only possible values of k, l satisfying (5-2) are listed in the table.

From the above, we know that T fixes a complex line polar to the vector $\boldsymbol{n}$. We draw the complex lines fixed by R, T, R_1, R_3, RR_3R^{-1} and TR_1T^{-1} respectively; see Figure 16. The orthogonality properties of these complex lines come from the braid relations. Thus the polyhedron can be constructed by following the same procedures as in the previous sections. A little modification occurs when dealing with the action of the stabilizer $\langle R, S\rangle$ on the complex line fixed by T, that is, a geodesic hyperbolic triangle $\triangle(k/2, p, p)$ with angles $2\pi/k, \pi/p, \pi/p$. As l tends to ∞, the complex line fixed by T degenerates to an ideal point. The action of the stabilizer $\langle R, S\rangle$ on the boundary is almost Euclidean, in other words, the triangle $\triangle(k/2, p, p)$ becomes a Euclidean triangle in a horizontal section of the Heisenberg group since $1/p + 1/k = 1/2$.

From the above arguments, the construction of fundamental domains for $\Gamma(3, k)$ can be implemented for all Mostow groups of the second type. Analogous to the case G_2 (that is conjugate to $\Gamma(3, 6)$), the limiting configuration of fundamental domains for $\Gamma(4, k)$ and $\Gamma(6, k)$ turns out to be two of the Mostow groups of the first type. In these cases, T becomes a parabolic element. The presentation may be

obtained by removing the relation $T^l = 1$. This gives a new approach to construct fundamental domains for some of the Mostow groups of the first type.

Acknowledgements

The author would like to thank John R. Parker for many motivating conversations and discussions related to calculations in complex hyperbolic geometry, specially for his explanations about the construction for Livné's groups during his visit to Durham University. Further thanks are due to James M. Thompson, who provided crucial inspiration when he was explaining his Ph.D. thesis. Finally, the author would like to express his deep thanks to the anonymous referee for a very detailed report that helped the author greatly improve the original proof.

References

[Deraux et al. 2005] M. Deraux, E. Falbel, and J. Paupert, "New constructions of fundamental polyhedra in complex hyperbolic space", *Acta Math.* **194**:2 (2005), 155–201. MR 2007h:32038 Zbl 1113.22010

[Falbel and Parker 2006] E. Falbel and J. R. Parker, "The geometry of the Eisenstein–Picard modular group", *Duke Math. J.* **131**:2 (2006), 249–289. MR 2007f:22011 Zbl 1109.22007

[Falbel et al. 2011] E. Falbel, G. Francsics, and J. R. Parker, "The geometry of the Gauss–Picard modular group", *Math. Ann.* **349**:2 (2011), 459–508. MR 2011k:22009 Zbl 1213.14049

[Giraud 1921] G. Giraud, "Sur certaines fonctions automorphes de deux variables", *Ann. Sci. École Norm. Sup.* (3) **38** (1921), 43–164. MR 1509233

[Goldman 1999] W. M. Goldman, *Complex hyperbolic geometry*, Clarendon, New York, 1999. MR 2000g:32029 Zbl 0939.32024

[Mostow 1980] G. D. Mostow, "On a remarkable class of polyhedra in complex hyperbolic space", *Pacific J. Math.* **86**:1 (1980), 171–276. MR 82a:22011 Zbl 0456.22012

[Mostow 1988] G. D. Mostow, "On discontinuous action of monodromy groups on the complex n-ball", *J. Amer. Math. Soc.* **1**:3 (1988), 555–586. MR 89h:22020 Zbl 0657.22014

[Parker 2006] J. R. Parker, "Cone metrics on the sphere and Livné's lattices", *Acta Math.* **196**:1 (2006), 1–64. MR 2007j:32021 Zbl 1100.57017

[Parker 2009] J. R. Parker, "Complex hyperbolic lattices", pp. 1–42 in *Discrete groups and geometric structures*, edited by K. Dekimpe et al., Contemp. Math. **501**, Amer. Math. Soc., Providence, RI, 2009. MR 2011g:22018 Zbl 1200.22004

[Parker and Paupert 2009] J. R. Parker and J. Paupert, "Unfaithful complex hyperbolic triangle groups, II: Higher order reflections", *Pacific J. Math.* **239**:2 (2009), 357–389. MR 2009h:20057 Zbl 1161.20046

[Sauter 1990] J. K. Sauter, Jr., "Isomorphisms among monodromy groups and applications to lattices in PU(1, 2)", *Pacific J. Math.* **146**:2 (1990), 331–384. MR 92d:22016 Zbl 0759.22013

[Thompson 2010] J. M. Thompson, *Complex hyperbolic triangle groups*, thesis, Durham University, Durham, 2010, Available at http://etheses.dur.ac.uk/478/1/thesis.pdf.

[Zhao 2011] T. Zhao, "A minimal volume arithmetic cusped complex hyperbolic orbifold", *Math. Proc. Cambridge Philos. Soc.* **150**:2 (2011), 313–342. MR 2012b:22012 Zbl 05862421

Received September 23, 2011. Revised March 21, 2012.

TIEHONG ZHAO
DEPARTMENT OF MATHEMATICS
HANGZHOU NORMAL UNIVERSITY
HANGZHOU, 310036
CHINA
tiehongzhao@gmail.com

PACIFIC JOURNAL OF MATHEMATICS

http://pacificmath.org

Founded in 1951 by
E. F. Beckenbach (1906–1982) and F. Wolf (1904–1989)

See inside back cover or pacificmath.org for submission instructions.

The subscription price for 2012 is US $420/year for the electronic version, and $485/year for print and electronic.
Subscriptions, requests for back issues from the last three years and changes of subscribers address should be sent to Pacific Journal of Mathematics, P.O. Box 4163, Berkeley, CA 94704-0163, U.S.A. Prior back issues are obtainable from Periodicals Service Company, 11 Main Street, Germantown, NY 12526-5635. The Pacific Journal of Mathematics is indexed by Mathematical Reviews, Zentralblatt MATH, PASCAL CNRS Index, Referativnyi Zhurnal, Current Mathematical Publications and the Science Citation Index.

The Pacific Journal of Mathematics (ISSN 0030-8730) at the University of California, c/o Department of Mathematics, 969 Evans Hall, Berkeley, CA 94720-3840, is published monthly except July and August. Periodical rate postage paid at Berkeley, CA 94704, and additional mailing offices. POSTMASTER: send address changes to Pacific Journal of Mathematics, P.O. Box 4163, Berkeley, CA 94704-0163.

PJM peer review and production are managed by EditFLOW™ from Mathematical Sciences Publishers.

PUBLISHED BY PACIFIC JOURNAL OF MATHEMATICS
at the University of California, Berkeley 94720-3840
A NON-PROFIT CORPORATION
Typeset in LaTeX

PACIFIC JOURNAL OF MATHEMATICS

Volume 259 No. 1 September 2012
